

## Supporting Information for: CO<sub>2</sub> Reduction by Fe(I): Solvent Control of C-O Cleavage versus C-C Coupling

Caroline T. Saouma,<sup>a</sup> Connie C. Lu,<sup>b</sup> Michael Day,<sup>a,c</sup> and Jonas C. Peters<sup>\*a</sup>

<sup>a</sup>Address: Division of Chemistry and Chemical Engineering, California Institute of Technology, Pasadena, California, 91125.

<sup>b</sup>Present Address: University of Minnesota, Department of Chemistry, Minneapolis, Minnesota, 55455, USA.

<sup>c</sup>Deceased.

<b>Experimental Section</b> .....	S-2
<b>Fig. S1.</b> Overlaid UV-Vis spectra of <b>1</b> in THF and MeCy.....	S-8
<b>Fig. S2.</b> Overlaid UV-Vis spectra of <b>1</b> + various equivalents of PCy <sub>3</sub> in THF.....	S-8
<b>Fig. S3.</b> X-band EPR spectrum of <b>1</b> .....	S-9
<b>Fig. S4.</b> <sup>1</sup> H NMR (300 MHz) spectrum of <b>1</b> (d <sub>14</sub> -MeCy).....	S-10
<b>Fig. S5.</b> <sup>1</sup> H NMR (400 MHz) spectrum of <b>3</b> (C <sub>6</sub> D <sub>6</sub> ).....	S-11
<b>Fig. S6.</b> <sup>1</sup> H NMR (300 MHz) spectrum of <b>7</b> (C <sub>6</sub> D <sub>6</sub> ).....	S-12
<b>Fig. S7.</b> <sup>1</sup> H NMR (400 MHz) spectrum of <b>8</b> (d <sub>8</sub> -THF).....	S-13
<b>Fig. S8.</b> <sup>1</sup> H NMR (300 MHz) spectrum of <b>12</b> (C <sub>6</sub> D <sub>6</sub> ).....	S-14
<b>Fig. S9.</b> <sup>1</sup> H NMR (300 MHz) spectrum of <b>14</b> (d <sub>8</sub> -THF).....	S-14
<b>Fig. S10.</b> <sup>1</sup> H NMR (300 MHz) spectrum of <b>15</b> (C <sub>6</sub> D <sub>6</sub> ).....	S-15
<b>Fig. S11.</b> <sup>1</sup> H NMR (300 MHz) spectrum of [PhBP <sup>CH<sub>2</sub>Cy</sup> <sub>3</sub> ]Fe(CO) <sub>2</sub> (C <sub>6</sub> D <sub>6</sub> ).....	S-16
<b>Fig. S12.</b> <sup>1</sup> H NMR profile (C <sub>6</sub> D <sub>6</sub> ) of the reaction between <b>12</b> and CO <sub>2</sub> .....	S-17
<b>Fig. S13.</b> 50% thermal ellipsoid representation of <b>14</b> .....	S-18
<b>Fig. S14.</b> [PhBP <sup>Me</sup> <sub>3</sub> ]Fe(CO) <sub>2</sub> (THF) <sub>x</sub> structures and spin-states that were investigated by DFT methods.....	S-19
<b>Fig. S15.</b> Theoretically predicted geometry and calculated spin-density for various Fe(CO) <sub>2</sub> (THF) <sub>x</sub> isomers.....	S-19
<b>Table S1.</b> Cartesian coordinates of the optimized geometry of [PhBP <sup>Me</sup> <sub>3</sub> ]Fe(η <sup>1</sup> -OCO) quartet.....	S-20
<b>Table S2.</b> Cartesian coordinates of the optimized geometry of [PhBP <sup>Me</sup> <sub>3</sub> ]Fe(η <sup>2</sup> -OCO) quartet.....	S-22
<b>Table S3.</b> Cartesian coordinates of the optimized geometry of [PhBP <sup>Me</sup> <sub>3</sub> ]Fe(η <sup>2</sup> -OCO) doublet.....	S-24
<b>Table S4.</b> Cartesian coordinates of the optimized geometry of [PhBP <sup>Me</sup> <sub>3</sub> ]Fe(η <sup>2</sup> -OCO)(THF) doublet.....	S-26
<b>Table S5.</b> Cartesian coordinates of the optimized geometry of [PhBP <sup>Me</sup> <sub>3</sub> ]Fe(η <sup>2</sup> -OCO)(THF) quartet.....	S-28
<b>Table S6.</b> Cartesian coordinates of the optimized geometry of [PhBP <sup>Me</sup> <sub>3</sub> ]Fe(η <sup>1</sup> -OCO)(THF) <sub>2</sub> doublet.....	S-30
<b>Table S7.</b> Mulliken atomic spin densities of the [PhBP <sup>Me</sup> <sub>3</sub> ]Fe(CO) <sub>2</sub> (THF) <sub>x</sub> species that could be satisfactorily minimized.....	S-32
<b>References</b> .....	S-33

## Experimental Section

### General Considerations

All manipulations were carried out using standard Schlenk or glove-box techniques under a dinitrogen atmosphere. Unless otherwise noted, solvents were deoxygenated and dried by sparging with N<sub>2</sub> followed by passage through an activated alumina column. Non-halogenated solvents were tested with a standard purple solution of benzophenone ketyl in THF to confirm effective oxygen and moisture removal. Deuterated solvents were purchased from Cambridge Isotopes Laboratories, Inc. and were degassed and stored over activated 3-Å molecular sieves prior to use. Elemental analyses were performed by Desert Analytics, Tucson, AZ, or by Midwest Microlab, Indianapolis, IN.

### Spectroscopic Methods

NMR data was collected at the MIT department of chemistry instrumentation facility or at the Caltech High-resolution NMR facility. Varian 300 MHz and 500 MHz and Bruker 400 MHz spectrometers were used to record the <sup>1</sup>H NMR and <sup>31</sup>P NMR spectra at ambient temperature. <sup>1</sup>H chemical shifts were referenced to residual solvent, while <sup>31</sup>P NMR chemical shifts were referenced to 85% H<sub>3</sub>PO<sub>4</sub> at δ 0 ppm. EPR data was collected at the MIT department of chemistry instrumentation facility and were carried out on a Bruker EMX spectrometer outfitted with 13" magnets, an ER 4102ST cavity and a newly upgraded Gunn diode microwave source producing X-band (8-10 GHz) radiation outfitted with a cryo-cooled cavity. Spectra were recorded in a methylcyclohexane glass at 4K, and the data were fit using winEPR.<sup>1</sup> IR measurements were obtained with a KBr solution cell or a KBr pellet using a Bio-Rad Excalibur FTS 3000 spectrometer controlled by Varian Resolutions Pro software set at 4 cm<sup>-1</sup> resolution. Solution magnetic moments were measured using Evans method;<sup>2</sup> for these measurements, concentrations were typically around 10 mM. Optical spectroscopy measurements were taken on a Cary 50 UV-Vis spectrophotometer using a 1 cm two-window quartz cell sealed with standard ground-glass joints or Teflon plugs.

The equilibrium between **1** and **8** was determined by UV-Vis spectroscopy. Solutions of **1** in THF (1.0 mM) and MeCy (1.4 mM) were prepared, as were solutions of PCy<sub>3</sub> in THF (19 mM) and MeCy (7.3 mM). Mixtures of these solutions and solvent were added to 4 mL cuvettes, such that the final concentration of Fe was fixed at 0.52 mM (THF) or 0.45 mM (MeCy), the final volume fixed at 4 mL, and the equivalents of PCy<sub>3</sub> varied from 0 to 10.1 (THF) or 0 to 11.6 (MeCy). It was assumed that upon addition of 10.1 equivalents of PCy<sub>3</sub> (THF) and 11.6 equivalents of PCy<sub>3</sub> (MeCy), **8** was the only detectible species in solution. Addition of more than ca. 12 equivalents of PCy<sub>3</sub> resulted in loss of the isosbestic point at 852 nm (THF), and observation of further spectral changes suggested that multiple species were present in solution. Assuming mass balance, the relative amounts of **1** and **8** were obtained by monitoring the absorbance at 650 nm (THF) and 390 nm (MeCy); these wavelengths were chosen as they provided the largest spectral changes in the respective solvents (THF: ε<sub>750(1)</sub> = 530 M<sup>-1</sup> cm<sup>-1</sup>, ε<sub>750(8)</sub> = 37 M<sup>-1</sup> cm<sup>-1</sup>; MeCy: ε<sub>390(1)</sub> = 2700 M<sup>-1</sup> cm<sup>-1</sup>, ε<sub>750(8)</sub> = 160 M<sup>-1</sup> cm<sup>-1</sup>).

In THF, addition of 1 equivalent of PCy<sub>3</sub> to **1** resulted in an equilibrium whereby ~ 57 % of the Fe was coordinated to PCy<sub>3</sub>; with 3.3 equivalents of PCy<sub>3</sub>, ~ 92 % of the Fe was coordinated to PCy<sub>3</sub>. From this, the binding constant, *K*, was estimated to be ~ 6000 M<sup>-1</sup> (*K* = [**8**]/[**1**][PCy<sub>3</sub>]). Thus, in a 20 mM THF solution of **1** and 1 equivalent of PCy<sub>3</sub>, ~ 91 % of the Fe is in the form of **8**. Exemplary data is shown in Fig. S2.

In MeCy, addition of 1 equivalent of PCy<sub>3</sub> to **1** resulted in an equilibrium whereby ~ 95 % of the Fe was coordinated to PCy<sub>3</sub>. From this, the binding constant, *K*, was estimated to be ~ 900,000 M<sup>-1</sup> (*K* = [**8**]/[**1**][PCy<sub>3</sub>]). Thus, in a 20 mM MeCy solution of **1** and 1 equivalent of PCy<sub>3</sub>, ~ 99 % of the Fe is in the form of **8**.

### X-ray Crystallography Procedures

Data were collected at the X-ray crystallography facility at Caltech or at the MIT department of chemistry X-ray diffraction facility. Low-temperature diffraction data were collected on a Siemens or Bruker Platform three-circle

diffractometer coupled to a Bruker-AXS Smart Apex CCD detector with graphite-monochromated Mo or Cu K $\alpha$  radiation ( $\lambda = 0.71073$  or  $1.54178$  Å, respectively), performing  $\varphi$ - and  $\omega$ -scans. The structures were solved by direct or Patterson methods using SHELXS<sup>3</sup> and refined against  $F^2$  on all data by full-matrix least squares with SHELXL-97.<sup>4</sup> Several of the structures are missing high angle data, making them only 89 - 94 % complete. The value of theta for which each dataset is complete is noted in the “refine\_special\_details” section of the .cif.

The structures were refined using established methods.<sup>5</sup> All non-hydrogen atoms were refined anisotropically. All hydrogen atoms were included into the model at geometrically calculated positions and refined using a riding model. The isotropic displacement parameters of all hydrogen atoms were fixed to 1.2 times the U value of the atoms they are linked to (1.5 times for methyl groups). Several of the structures reported suffered from disorder in parts of the [PhBP<sup>R</sup><sub>3</sub>] ligand and/or disorder of solvent molecules (some over more than two independent positions). All disorders were refined with the help of similarity restraints on 1-2 and 1-3 distances and displacement parameters as well as rigid bond restraints for anisotropic displacement parameters. All close contacts, both inter and intramolecular, reported by the Platon validation software<sup>6</sup> involve at least one partner from a minor component of a disorder. While it is conceivable that more components of the molecule(s) are disordered and parameterization of these disordered components would remove the close contacts, the data at hand did not allow for further modeling of the disorder. The unit cell of **15** contains 8 THF molecules which have been treated as a diffuse contribution to the overall scattering without specific atom positions by SQUEEZE/PLATON. Specific refinement details for each structure are included in the .cif file.

### DFT Methods

Density functional calculations were carried out using the Gaussian 03 suite<sup>7</sup> using the unrestricted B3LYP functional. The 6-31++g(d,p) basis set was used for all single point energy and frequency calculations, and either 6-31++g(d,p) or TZVP/SV were used for geometry optimizations. For geometry optimizations, initial coordinates were taken from the solid-state structures of [PhBP<sup>CH<sub>2</sub>Cy</sup><sub>3</sub>]Fe(PMe<sub>3</sub>). Calculations were performed with a truncated tris(phosphino)borate ligand, whereby the cyclohexylmethyl substituents were replaced by methyl groups; initial calculations that employed the full ligand suggested that our DFT methods could not faithfully reproduce the conformational flexibility of the ligand's cyclohexylmethyl groups.

Geometry optimizations were carried out on [PhBP<sup>Me</sup><sub>3</sub>]Fe(CO<sub>2</sub>)(THF)<sub>x</sub>, where x = 0, 1, or 2, in both the doublet and quartet states, with the CO<sub>2</sub> bound either ( $\eta^2$ -OCO) or ( $\eta^1$ -OCO), for a total of 10 structures (see Fig. S14). Both the  $S = 1/2$  and  $3/2$  Fe( $\eta^1$ -OCO)(THF) species could be minimized, but the resulting structures had a linear CO<sub>2</sub> molecule ca. 5 Å away from the Fe center. As two imaginary vibrations were associated with the CO<sub>2</sub> in these structures, they were not considered viable intermediates. Both  $S = 1/2$  Fe( $\eta^1$ -OCO) and  $S = 3/2$  Fe( $\eta^1$ -OCO)(THF)<sub>2</sub> suffered from spin contamination,<sup>8</sup> and their geometries could not be minimized despite trying several basis sets/levels of theory. The remaining structures could be minimized; subsequent frequency analysis indicated the absence of imaginary frequencies. Molecular orbital plots were generated using GaussView 4.1<sup>9</sup> with isocontour values of 0.002 (density). See below for comparison of the structures.

### Starting Materials and Reagents

Compounds **1**, **4**, **13**, {[PhBP<sup>Pr</sup><sub>3</sub>]Fe}<sub>2</sub>( $\mu$ -N<sub>2</sub>), and [PhBP<sup>R</sup><sub>3</sub>]FeCl (R = Ph, <sup>i</sup>Pr, CH<sub>2</sub>Cy, *mter*), were prepared according to literature procedures.<sup>10</sup> All other reagents were purchased from commercial vendors and used without further purification.

### Synthesis and Characterization of Complexes

**Further characterization of 1.** UV-Vis (methylcyclohexane)  $\lambda_{\text{max}}$ , nm ( $\epsilon$ , M<sup>-1</sup> cm<sup>-1</sup>): 350 (sh, 3110), 390 (sh, 2700), 690 (220), 920 (sh, 290). UV-Vis (THF)  $\lambda_{\text{max}}$ , nm ( $\epsilon$ , M<sup>-1</sup> cm<sup>-1</sup>): 744 (585), 1024 (415). Evans Method ( $d_{14}$ -methylcyclohexane): 2.3  $\mu_B$ . IR (MeCy): 2056 cm<sup>-1</sup>.

### Synthesis of $\{[\text{PhBP}^{\text{CH}_2\text{Cy}}_3\text{Fe}]_2(\mu\text{-}\kappa\text{OO}':\kappa\text{OO}'\text{-oxalate}), \mathbf{3}$ .

- 1) Sodium amalgam (0.48 wt %, 1.12 mmol) and a magnetic stir bar were added to a frozen solution of  $[\text{PhBP}^{\text{CH}_2\text{Cy}}_3\text{FeCl}]$  (0.4013 g, 0.447 mmol) in 20 mL THF in a 100 mL Schlenk tube fitted with a Teflon valve. The vessel was evacuated, and allowed to warm to 0 °C in an acetone bath followed by an ice bath. One atmosphere of CO<sub>2</sub> was added, and the reaction was slowly stirred. The color changed from yellow to red/brown over 2.5 h, at which point the vessel was degassed. The solution was filtered through a thick Celite plug, and the remaining solids generously washed with benzene. The resulting solution was concentrated to a solid under partial vacuum. The resulting solids were extracted into 50 mL of benzene, filtered through Celite, and again concentrated to a solid under partial vacuum. The solid was washed with petroleum ether, extracted into benzene, and filtered through Celite. The resulting solution was lyophilized to give a red/brown solid (0.202 g, 50.1 %). Crystals suitable for X-ray diffraction can be grown from a THF/petroleum ether solution at -35 °C.
- 2) A solution of  $[\text{PhBP}^{\text{CH}_2\text{Cy}}_3\text{FeCl}]$  (0.5647 g, 0.6293 mmol) and PCy<sub>3</sub> (0.2001 g, 0.6922 mmol) in 20 mL THF was added to an Na/Hg amalgam (39.4 wt %, 0.7449 mmol), and subsequently stirred for 2 h. The reaction was filtered through a Celite-lined frit, diluted to 30 mL (ca. 20 mM), and transferred to a 100 mL Schlenk tube fitted with a stir bar and Teflon plug. The vessel was attached to a calibrated bulb (56.30 mL), and the solution frozen with liquid N<sub>2</sub>. After evacuating the headspace, CO<sub>2</sub> was added to the bulb and condensed (2 x 51.3 cm Hg, 3.15 mmol) into the reaction vessel. The reaction was warmed to room temperature and stirred for 24 h, during which the solution changed color from yellow to red-brown. The volatiles were removed and the resulting solids were triterated with pentane and collected on a frit. The pentane was concentrated, and the remaining solids were extracted into minimal THF. Both fractions were cooled to -35°C, allowing for **3** to crystallize out (pentane: 0.1504 g, 26.5 %; THF: 0.2182 g, 38.5 %).

<sup>1</sup>H NMR (C<sub>6</sub>D<sub>6</sub>, 300 MHz): δ 25.3, 14.9, 13.5, -0.5, -0.7, -1.29, -1.5, -2.7, -3.3, -3.7, -4.4, -6.2 (bs), -17.7 (bs). IR (KBr): 1644 cm<sup>-1</sup>. UV-Vis (C<sub>6</sub>H<sub>6</sub>) λ<sub>max</sub>, nm (ε, M<sup>-1</sup> cm<sup>-1</sup>): 775 (1000), 480 (sh, 760), 400 (sh, 1600), 330 (2600). Evans Method (C<sub>6</sub>D<sub>6</sub>): 4.3 μ<sub>B</sub>. Anal. Calc'd. for C<sub>104</sub>H<sub>178</sub>B<sub>2</sub>Fe<sub>2</sub>O<sub>4</sub>P<sub>6</sub>: C 68.95; H 9.90; N 0. Found: C 68.42; H 9.31; N <0.05.

**Synthesis of  $\{[\text{PhBP}^{\text{CH}_2\text{Cy}}_3\text{Fe}]_2(\mu\text{-}\eta^5:\eta^5\text{-1,1'-bicyclohexadienyl}), \mathbf{5}$ .** A 5 mL benzene solution of **4** (0.050 g, 27.75 μmol) was heated at 60 °C for 20 h. The solution changed from dark green to yellow with precipitation of orange microcrystals. Solids were collected and washed with petroleum ether, benzene, and THF (0.048 g, 92% yield). Single crystals suitable for X-ray diffraction can be grown from vapor diffusion of petroleum ether into a dichloromethane solution. <sup>1</sup>H NMR (CDCl<sub>3</sub>, 500 MHz): δ 7.33 (m, 4H, H<sub>o</sub> of Ph), 7.20 (t, 4H, *J* = 7.5 Hz, H<sub>m</sub> of Ph), 7.02 (t, 2H, *J* = 7.0 Hz, H<sub>p</sub> of Ph), 5.48 (br s, 2H), 4.15 (br s, 4H), 2.12 (br s, 4H), 1.99 (m, 12H), 1.75 – 1.66 (84H), 1.32 – 0.97 (62 H), 0.38 (br s, 12H). <sup>31</sup>P NMR (121 MHz, CD<sub>2</sub>Cl<sub>2</sub>): δ 44.5 (br) ppm. Anal. Calc'd. for C<sub>114</sub>H<sub>190</sub>B<sub>2</sub>Fe<sub>2</sub>P<sub>6</sub>: C 72.84; H 10.19; N 0. Found: C 72.65; H 9.77; N <0.05.

**Synthesis of  $\{[\text{PhBP}^{\text{CH}_2\text{Cy}}_3\text{Fe}]_2(\mu\text{-}\eta^5:\eta^5\text{-azobenzene}), \mathbf{6}$ .** To a 10 mL THF solution of **1** (0.1178 mmol), azobenzene (10.7 mg, 58.7 μmol) was added, and the reaction was stirred for 2 h. The dark-red solution was concentrated under reduced pressure to dryness. The residue was washed with petroleum ether and ether until the washings were nearly colorless. The residue was then extracted with dichloromethane and concentrated under reduced pressure to a red powder (0.075 g, 38% yield). Single crystals suitable for X-ray diffraction can be grown from vapor diffusion of diethyl ether into a dichloromethane solution. <sup>1</sup>H NMR (300 MHz, CDCl<sub>3</sub>): δ 7.31 (d, *J* = 7.5 Hz, 2H), 7.20 (t, *J* = 7.5 Hz, 2H), 7.04 (t, *J* = 7.5 Hz, 1H), 5.07 (m, 2H), 4.91 (m, 1H), 4.45 (m, 1H), 3.81 (m, 1H), 1.97 (m, 6H), 1.73 - 1.67 (m, 42H), 1.26 – 0.99 (m, 30H), 0.44 (br s, 6H). <sup>13</sup>C NMR (126 MHz, CDCl<sub>3</sub>): δ 166.2 (br), 146.4, 131.8, 127.3, 123.5, 96.0, 95.0, 69.6, 68.1, 62.2, 43.1 (br), 40.9 (br), 37.6, 37.2, 37.1, 36.0, 35.8,

27.4, 27.1, 26.8, 14.3 (br m).  $^{31}\text{P}$  NMR (121 MHz,  $\text{CD}_2\text{Cl}_2$ ):  $\delta$  47.4 ppm. UV-Vis ( $\text{C}_6\text{H}_6$ )  $\lambda_{\text{max}}$ , nm ( $\epsilon$ ,  $\text{M}^{-1}\text{cm}^{-1}$ ): 465 (19,700), 324 (35,500). Anal. Calc'd. for  $\text{C}_{114}\text{H}_{188}\text{B}_2\text{Fe}_2\text{N}_2\text{P}_6$ : C 71.84; H 9.94; N 1.47. Found: C 72.13; H 9.64; N 1.57.

**Synthesis of  $[\text{PhBP}^{\text{CH}_2\text{Cy}}_3]\text{FePPh}_3$ , 7.** Triphenylphosphine (0.0963 g, 0.367 mmol) was added as a solid to a stirring solution of **1** (0.3295 g, 0.367 mmol) in 20 mL of THF. The reaction mixture was stirred for 20 minutes, during which the color changed from lime green to dark orange. The solution was concentrated under reduced pressure to dryness. The solids were extracted with benzene, and filtered through a glass wool pipette. The solution was concentrated under reduced pressure to give analytically pure solids (0.3369 g, 82 %). Single crystals suitable for X-ray diffraction can be grown from a benzene/petroleum ether mixture at  $-35^\circ\text{C}$ .  $^1\text{H}$  NMR ( $d_8$ -THF, 300 MHz):  $\delta$  54 (bs), 13.3, 9.7, 8.6, 7.9, 7.3, 7.0, 4.7, 3.5, 3.4, 2.6, 2.3, 1.9, 1.9, 1.7, 1.5, 1.1, -1.0, -8 (bs). UV-Vis (THF)  $\lambda_{\text{max}}$ , nm ( $\epsilon$ ,  $\text{M}^{-1}\text{cm}^{-1}$ ): 470 (sh, 780), 365 (2900), 260 (sh, 12800). Evans Method ( $\text{C}_6\text{D}_6$ ): 4.2  $\mu\text{B}$ . Anal. Calc'd. for  $\text{C}_{69}\text{H}_{104}\text{BFeP}_4$ : C 73.72; H 9.33; N 0. Found: C 73.56; H 9.14; N 0.

**Synthesis of  $[\text{PhBP}^{\text{CH}_2\text{Cy}}_3]\text{FePCy}_3$ , 8.** A solution of  $[\text{PhBP}^{\text{CH}_2\text{Cy}}_3]\text{FeCl}$  (0.1070 g, 0.119 mmol) in 10 mL of THF was added to Na/Hg (0.39 wt %, 0.183 mmol). The reaction stirred for 1.5 h, during which time the color changed from yellow to pale green. The solution was decanted off of the amalgam, solid  $\text{PCy}_3$  was added to the solution (0.0334 g, 0.119 mmol), and after stirring for 10 minutes, the volatiles were removed under reduced pressure. The residue was then triturated with pentane and the solids extracted into MeCy. The MeCy solution was filtered through a Celite-lined frit, and the volatiles were removed under reduced pressure (0.1300g, 96 %).  $^1\text{H}$  NMR ( $d_8$ -THF, 300 MHz):  $\delta$  50 (bs), 9.7, 8.2, 7.9, 7.3, 7.1, 6.1, 3.2, 2.9, 2.6, 1.0, -1.7 (bs), -9.4 (bs). UV-Vis spectrum was taken in the presence of 10.1 equiv of  $\text{PCy}_3$  (THF) or 11.6 equiv of  $\text{PCy}_3$  (MeCy). UV-Vis (THF)  $\lambda_{\text{max}}$ , nm ( $\epsilon$ ,  $\text{M}^{-1}\text{cm}^{-1}$ ): 1000 (875), 1091 (sh, 1041). UV-Vis (MeCy)  $\lambda_{\text{max}}$ , nm ( $\epsilon$ ,  $\text{M}^{-1}\text{cm}^{-1}$ ): 1000 (945), 1091 (sh, 1065). Evans Method ( $d_8$ -THF): 3.9  $\mu\text{B}$ . Anal. Calc'd. for  $\text{C}_{69}\text{H}_{122}\text{BFeP}_4$ : C 72.55; H 10.76; N 0. Found: C 72.39; H 10.59; N 0.

**Synthesis of  $\{[\text{PhBP}^{\text{CH}_2\text{Cy}}_3]\text{Fe}(\text{CO})\}_2(\mu\text{-}\kappa\text{OO}'\text{:}\kappa\text{OO}'\text{-oxalate})$ , 9.**  $\{[\text{PhBP}^{\text{CH}_2\text{Cy}}_3]\text{Fe}\}_2(\mu\text{-oxalate})$  (**3**) (0.0612 g, 0.033 mmol) was dissolved in 15 mL of THF and transferred to a 25 mL Schlenk tube fitted with a stir bar. The tube was attached to a calibrated bulb (3.89  $\text{cm}^3$ ) which was attached to a Schlenk line. The vessel and bulb were evacuated and the reaction vessel was placed in a dry ice/acetone bath. CO was added to the bulb (35 cm Hg, 0.074 mmol) and the gas was introduced to the stirring solution. The color of the reaction changed from brown to rose-red over 2 h. Volatiles were removed under reduced pressure. The resulting solids were extracted into benzene, filtered through Celite, and lyophilized to give a brown solid (0.0527 g, 82.4 %). Crystals suitable for X-ray diffraction can be grown from toluene at  $-35^\circ\text{C}$ .  $^1\text{H}$  NMR ( $\text{C}_6\text{D}_6$ , 300 MHz):  $\delta$  7.91 (d,  $J = 7.5$  Hz), 7.51 (t,  $J = 7.5$  Hz), 7.24 (t), 1.0-2.5 (m).  $^{31}\text{P}$  NMR ( $\text{C}_6\text{D}_6$ , 121.4 MHz):  $\delta$  50.81 (d,  $^2J_{\text{PP}} = 67.7$  Hz, 4P), 25.09 (t,  $^2J_{\text{PP}} = 67.7$  Hz, 2P). IR (KBr): 1945, 1634  $\text{cm}^{-1}$ . UV-Vis (THF)  $\lambda_{\text{max}}$ , nm ( $\epsilon$ ,  $\text{M}^{-1}\text{cm}^{-1}$ ): 548 (270), 398 (sh, 2200), 293 (7900), 245 (19,800). Anal. Calc'd. for  $\text{C}_{106}\text{H}_{178}\text{B}_2\text{Fe}_2\text{O}_6\text{P}_6$ : C 68.17; H 9.61; N 0. Found: C 67.48; H 9.35; N < 0.05.

**Synthesis of  $\{[\text{PhBP}^{\text{iPr}}_3]\text{Fe}\}_2(\mu\text{-O})$ , 10.** Solid  $[\text{PhBP}^{\text{iPr}}_3]\text{FeCl}$  (0.2553 g, 0.446 mmol), sodium amalgam (0.48 wt %, 1.17 mmol), and a stir bar were transferred to a 25 mL Schlenk tube fitted with a Teflon valve. THF (13 mL) was vac-transferred onto the solids, and the yellow solution was warmed to  $0^\circ\text{C}$  in an acetone bath followed by an ice bath. An atmosphere of  $\text{CO}_2$  was added to the vessel, and the reaction was stirred slowly for 2 h to give a red solution. The ice bath was removed, and the reaction was vigorously stirred for an additional 2 h before being degassed. The solution was filtered through Celite and the volatiles removed. The remaining solids were extracted into benzene, filtered, and lyophilized. The solids were washed with petroleum ether, and the remaining solids crystallized from THF in a vapor diffusion chamber containing MeCy (0.0368 g, 15.2 %). Crystals suitable for diffraction can be grown via vapor diffusion of petroleum ether into a benzene solution.  $^1\text{H}$  NMR ( $\text{C}_6\text{D}_6$ , 300 MHz):  $\delta$  27.3, 15.6, 10.8, 10.0 (t,  $J = 6$  Hz), -0.26, -5.1. UV-Vis (THF)  $\lambda_{\text{max}}$ , nm ( $\epsilon$ ,  $\text{M}^{-1}\text{cm}^{-1}$ ): 948 (180), 624 (sh, 120), 535

(sh, 390), 470 (sh, 910). Evans Method ( $C_6D_6$ ): 2.8  $\mu_B$ . Anal. Calc'd. for  $C_{54}H_{106}B_2Fe_2OP_6$ : C 59.46; H 9.80; N 0. Found: C 59.37; H 9.61; N < 0.05.

**Synthesis of  $[PhBP^{iPr}_3]Fe(CO)_2$ , **11**.**  $\{[PhBP^{iPr}_3]Fe\}_2(\mu-N_2)$  (0.0775 mmol, 0.070 mmol) was dissolved in 5 mL benzene, and transferred to a 25 mL Schlenk tube fitted with a Teflon valve. The vessel was evacuated, and an atmosphere of CO was introduced to the brown solution. After 20 min, the light brown solution was degassed and lyophilized. The resulting solids were crystallized in minimal toluene stored at  $-35\text{ }^\circ\text{C}$  (0.0673 mg, 72.9 %).  $^1H$  NMR ( $C_6D_6$ , 300 MHz):  $\delta$  8.4, 7.8, 7.6, 5.3 (bs), 1.2, -1.3 (bs). IR (KBr): 1955, 1888  $cm^{-1}$  UV-Vis (THF)  $\lambda_{max}$ , nm ( $\epsilon$ ,  $M^{-1} cm^{-1}$ ): 460 (sh, 854), 400 (sh, 1800), 311 (15000). Evans Method ( $C_6D_6$ ): 1.73  $\mu_B$ . Anal. Calc'd. For  $C_{29}H_{53}BFeO_2P_3$ : C 58.71; H 9.00; N 0. Found: C 58.40; H 8.96; N < 0.05.

**Synthesis of  $\{[PhBP^{Ph}_3]Fe\}_2(\mu-O)$ , **12** and  $[PhBP^{Ph}_3]Fe(CO)_2Na(THF)_5$ , **14**.** Solid  $[PhBP^{Ph}_3]FeCl$  (0.1712 g, 0.22 mmol) and sodium amalgam (0.46 wt %, 0.587 mmol) was transferred to a 25 mL Schlenk tube fitted with a Teflon valve. THF (13 mL) was vac-transferred onto the solids, and the solution was warmed to  $0\text{ }^\circ\text{C}$  in an acetone bath followed by an ice bath, at which time 1 atmosphere of  $CO_2$  was introduced to the vessel. The reaction was stirred slowly for 1 h, then vigorously for 3 h. The orange/brown solution was degassed, filtered through Celite, and the volatiles were removed under partial pressure. The solids were extracted into benzene and filtered through Celite (**12**). The remaining benzene insoluble orange solids (**13**) were extracted into THF, and volatiles were removed from both solutions.

The benzene extract (**12**) was re-extracted into benzene, filtered, and lyophilized. The solids were washed with MeCy, and triply re-crystallized by layering pentane over a benzene solution to afford **12**.  $^1H$  NMR ( $C_6D_6$ , 300 MHz):  $\delta$  25.6 (s), 14.6 (d,  $J = 6$  Hz), 10.41 (t,  $J = 6$  Hz), 9.73 (t,  $J = 7.5$  Hz), 5.17 (s), 4.22 (t,  $J = 6$  Hz), 2.87 (s). UV-Vis (THF)  $\lambda_{max}$ , nm ( $\epsilon$ ,  $M^{-1} cm^{-1}$ ): 896 (240), 653 (sh, 250), 555 (sh, 520), 491 (sh, 1270). Evans Method ( $C_6D_6$ ): 2.8  $\mu_B$ . Anal. Calc'd. for  $C_{90}H_{82}B_2Fe_2OP_6$ : C 72.12; H 5.51; N 0. Found: C 71.70; H 5.96; N < 0.05.

The benzene-insoluble solids (**14**) were re-extracted into THF, filtered through Celite. Crystals suitable for XRD were grown by layering a THF solution of **14** with at  $-35\text{ }^\circ\text{C}$ . (17.0 mg, 6.4 %).  $^1H$  NMR ( $d_8$ -THF, 300 MHz):  $\delta$  7.53 (s), 7.37 (s), 7.06 (t,  $J = 6.1$  Hz), 6.83 (s), 3.61, 1.77, 1.26 (bs).  $^{31}P$  NMR ( $d_8$ -THF, 121.4 MHz):  $\delta$  57.0. IR (KBr): 1870, 1781  $cm^{-1}$ . UV-Vis (THF)  $\lambda_{max}$ , nm ( $\epsilon$ ,  $M^{-1} cm^{-1}$ ): 335 (5600). Anal. Calc'd. for  $C_{67}H_{81}BFeNaO_7P_3$ : C 68.14; H 6.91; N 0. Found: C 68.16; H 6.71; N 0.

**Alternative Synthesis of  $[PhBP^{Ph}_3]Fe(CO)_2Na(THF)_5$ , **14**:** A solution of **13** (0.4363 g, 0.547 mmol) in 20 mL THF was added to a sodium/mercury amalgam (0.40 wt %, 0.602 mmol) and was stirred for 2 h. The reaction was filtered through a Celite-lined frit, and volatiles were removed. The resulting solids were washed with petroleum ether, extracted into THF, and filtered through Celite. Volatiles were removed under reduced pressure to give an orange/red powder (0.3405 g, 0.288 mmol, 53 %).

**Synthesis of  $\{[PhBP^{Ph}_3]Fe\}(\mu-\eta^1:\eta^2\text{-carbonate})$ , **15**:** A solution of **12** (7.5 mg, 0.005 mmol) in 1 mL of  $C_6D_6$  was transferred to a resealable j.young NMR tube. On a Schlenk-line, the solution was frozen with liquid nitrogen and the headspace was evacuated. The vessel was warmed to room temperature and an atmosphere of  $CO_2$  was added to the tube. The reaction stirred for 1 h at  $60\text{ }^\circ\text{C}$ , during which time clean and quantitative conversion to **15** occurs, as noted by a single set of paramagnetically shifted resonances in the  $^1H$  NMR spectrum. Upon exposure to an  $N_2$  atmosphere or vacuum, solutions of **15** revert to **12**, precluding our ability to obtain analytically pure material in the solid-state. Crystals of **15** suitable for diffraction were obtained by layering a THF solution of **15** with pentane at  $-35$

°C.  $^1\text{H}$  NMR ( $\text{C}_6\text{D}_6$ , 300 MHz):  $\delta$  120 (bs), 28.6, 15.7, 14.6, 6.2, -4.2, -13 (bs). IR ( $\text{C}_6\text{D}_6/\text{KBr}$ ):  $1470\text{ cm}^{-1}$ . Evans Method ( $\text{C}_6\text{D}_6$ ):  $5.8\ \mu\text{B}$ .

A sample of  $^{13}\text{C}$ -enriched **15** was prepared following the above procedure with  $^{13}\text{CO}_2$ . IR ( $\text{C}_6\text{D}_6/\text{KBr}$ ):  $1455\text{ cm}^{-1}$ .

**Synthesis of  $[\text{PhBP}^{\text{CH}_2\text{Cy}}_3]\text{Fe}(\text{CO})_2$ .** A solution of **1** (0.147 mmol, 0.015 M) was transferred to a 50 mL schlenk tube fitted with a Teflon plug, and cooled to  $-78\text{ }^\circ\text{C}$ . The tube was attached to a calibrated bulb that contained two equivalents of CO (56.4 mL, 9.6 cm Hg), and the tube opened to the bulb. The reaction stirred for 18 h during which it warmed to room temperature and changed color from lime green to dark orange. Volatiles were removed under partial pressure, and the resulting solids were extracted into benzene and filtered through Celite. The benzene solution was concentrated under reduced pressure. The solids were taken up in minimal pentane, and stored at  $-35\text{ }^\circ\text{C}$  to give crystals of  $[\text{PhBP}^{\text{CH}_2\text{Cy}}_3]\text{Fe}(\text{CO})_2$ . (64.7 mg, 47.6 %).  $^1\text{H}$  NMR ( $\text{C}_6\text{D}_6$ , 300 MHz):  $\delta$  8.1 (bs), 7.8, 7.4, 7.05, 2.0 (bs), 1.2 (bs). IR (KBr):  $1959, 1894\text{ cm}^{-1}$ . UV-Vis (THF)  $\lambda_{\text{max}}$ , nm ( $\epsilon$ ,  $\text{M}^{-1}\text{ cm}^{-1}$ ): 410 (2130), 355 (sh, 1600), 295 (sh, 4540), 253 (sh, 8300). Evans Method ( $\text{C}_6\text{D}_6$ ):  $1.73\ \mu\text{B}$ . Anal. Calc'd. for  $\text{C}_{53}\text{H}_{89}\text{BFeO}_2\text{P}_3$ : C 69.35; H 9.77; N 0. Found: C 69.23; H 9.49; N 0.

**Reaction Studies Between  $[\text{PhBP}^{\text{CH}_2\text{Cy}}_3]\text{Fe}(\text{PR}'_3)$  and  $\text{CO}_2$ .** In a typical reaction, a 20 mM solution of  $[\text{PhBP}^{\text{CH}_2\text{Cy}}_3]\text{Fe}(\text{PR}_3)$  (0.02 mmol) was transferred to a 15 mL Schlenk tube fitted with a Teflon plug and a stir bar. The vessel was attached to a calibrated bulb which was attached to a Schlenk-line. The line was flushed 3 times with  $\text{CO}_2$ , and the tip of the vessel was cooled with liquid nitrogen. The vessel was then evacuated, and ten equivalents of  $\text{CO}_2$  was loaded into the calibrated bulb, which was then condensed into the vessel with liquid nitrogen. The reaction was allowed to stir for 24 h prior to removal of the volatiles. The solids were dissolved in  $700\ \mu\text{L}$  of a standard  $\text{C}_6\text{D}_6$  solution containing 10 mM  $\text{P}^t\text{Bu}_3$  and transferred to a j.young resealable NMR tube, saving an aliquot for IR analysis ( $\text{P}^t\text{Bu}_3$  does not bind **1**). Both  $^1\text{H}$  and  $^{31}\text{P}$  NMR spectra were collected, and peaks corresponding to **2**,  $\text{P}^t\text{Bu}_3$ , and  $\text{PR}_3$  were integrated. The sample was then freeze-pump-thawed on a Schlenk-line and an atmosphere of CO was introduced. The NMR tube was sealed and mechanically rotated for an hour prior to repeating the NMR analysis. Now in the  $^{31}\text{P}$  NMR spectra peaks corresponding to **2**, **9**,  $\text{P}^t\text{Bu}_3$ , and  $\text{PR}_3$  were integrated. The corresponding  $^1\text{H}$  NMR spectrum showed no paramagnetic peaks associated with **3**, indicating complete conversion to **9** (this was also confirmed by the mass balance obtained from the integration of the  $^{31}\text{P}$  NMR signals). For some reactions, a second IR spectrum was taken after the NMR analysis (this also confirmed full conversion of **3** to **9**).

Reactions between **4** and  $\text{CO}_2$  were similarly analyzed.

**Reaction of **12** with CO.** A solution of **12** (0.0244 g, 0.016 mmol) in 3 mL THF was prepared and transferred to a 15 mL Schlenk tube fitted with a stir bar and Teflon plug. The vessel was evacuated and an atmosphere of CO introduced. The reaction stirred for 2 hours, during which time a color change from brown to tan was observed. The volatiles were removed, and the resulting solids were taken up in  $\text{C}_6\text{D}_6$  and the solution analyzed by  $^1\text{H}$  and  $^{31}\text{P}$  NMR spectroscopy. No peaks were present in the  $^{31}\text{P}$  spectrum. In the  $^1\text{H}$  NMR spectrum, the characteristic paramagnetic peaks of **12** were absent, and the only resonances present were those corresponding to  $[\text{PhBP}^{\text{Ph}}_3]\text{Fe}(\text{CO})_2$ .<sup>10c</sup> The volatiles of the  $\text{C}_6\text{D}_6$  solution were removed, and the resulting solids were analyzed by IR spectroscopy (KBR pellet). Resonances ascribed to  $[\text{PhBP}^{\text{Ph}}_3]\text{Fe}(\text{CO})_2$  were present in the carbonyl stretching region.

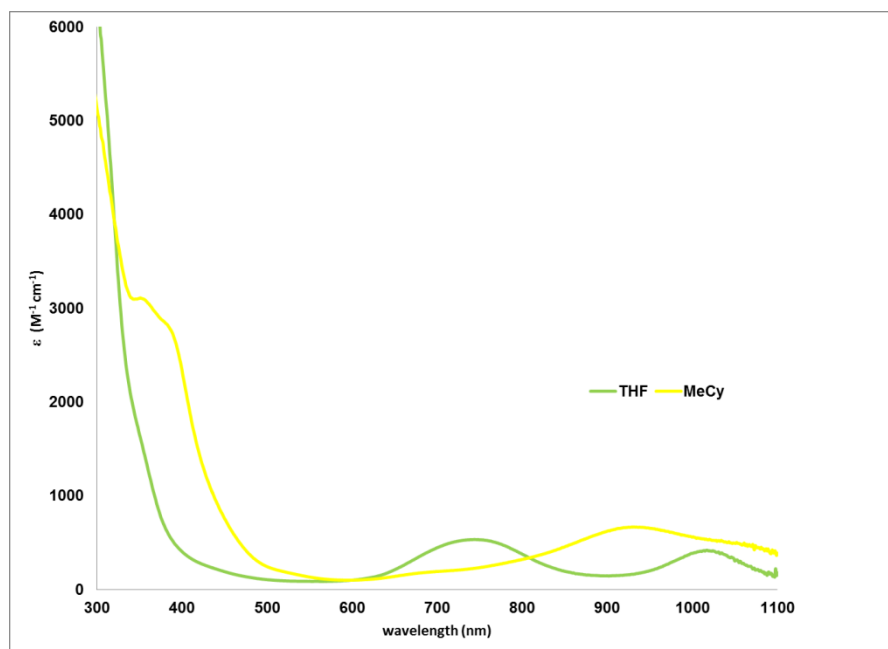


**Fig. S1.** Overlaid UV-Vis spectra of **1** in THF and MeCy.

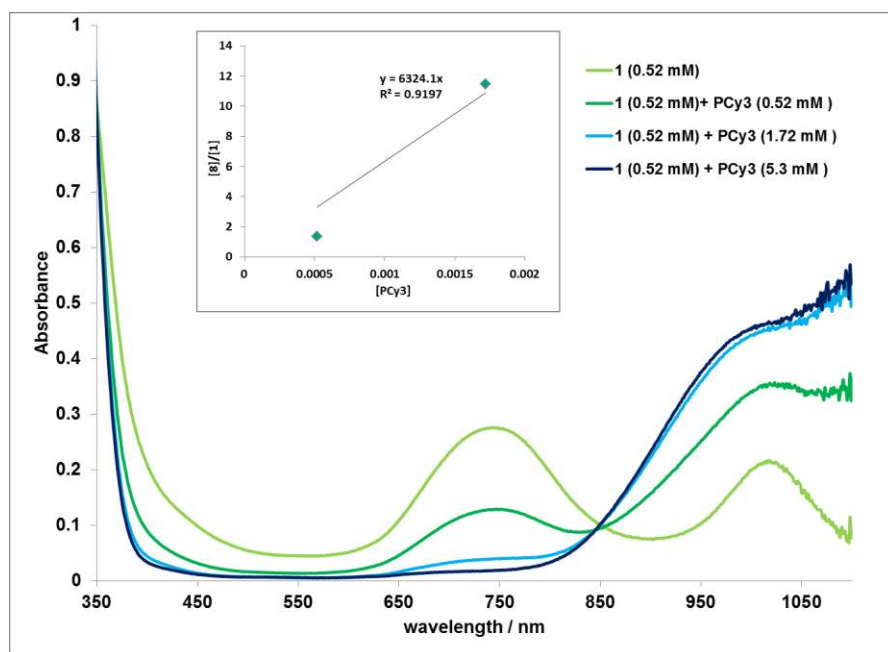


**Fig. S2.** Overlaid UV-Vis spectra of 0.52 mM solutions of **1** in THF, with 0 – 5.3 mM PCy<sub>3</sub>. Inset: Plot of  $[PCy_3]$  vs.  $[8]/[1]$ . The slope of  $\sim 6000 \text{ M}^{-1}$  corresponds to  $K$ .



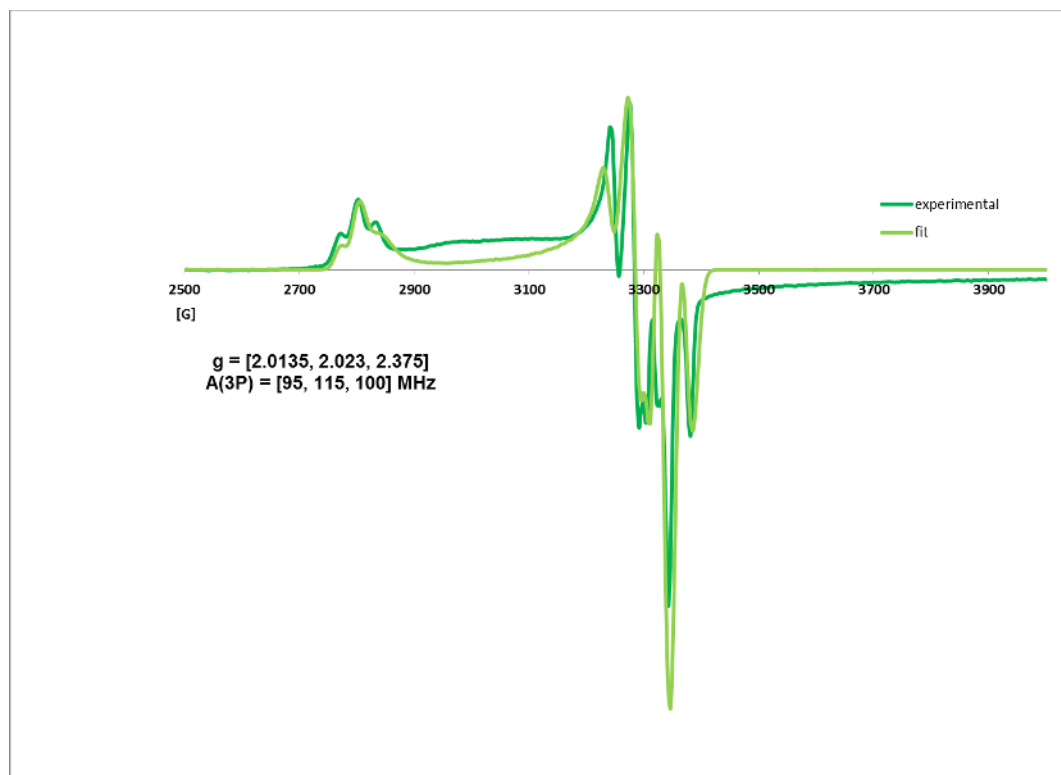


**Fig. S3.** X-band EPR spectrum of **1** (Gauss) recorded at 4K in a MeCy glass (experimental dark green; fit light green).

car3219\_5

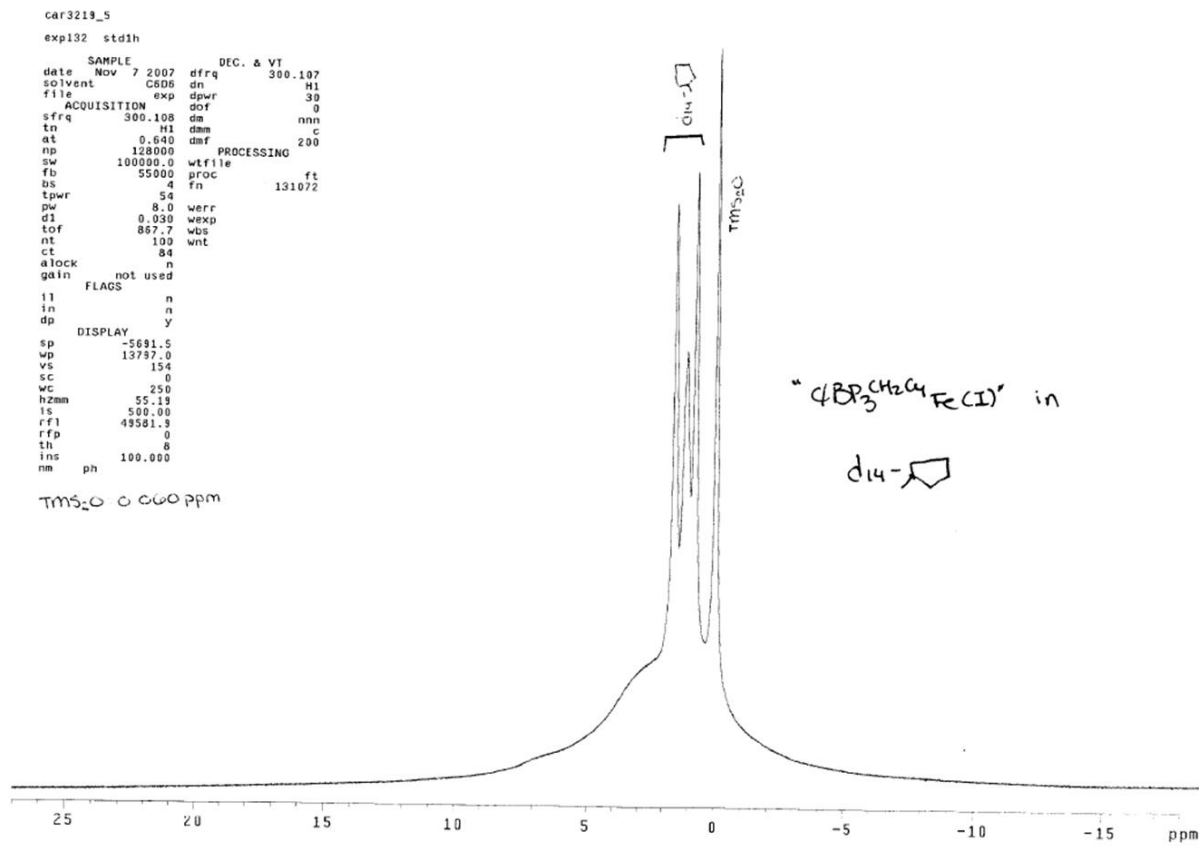


Fig. S4. <sup>1</sup>H NMR (300 MHz) spectrum of **1** (d<sub>14</sub>-MeCy).

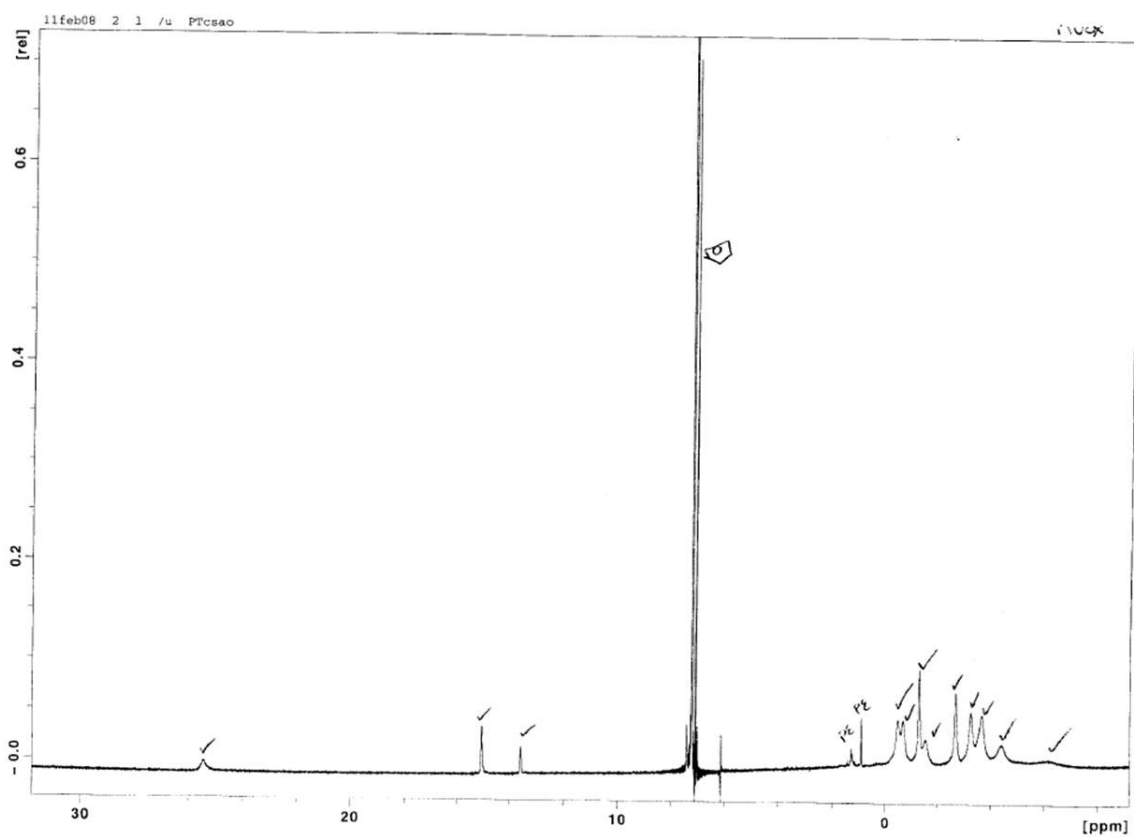


Fig. S5. <sup>1</sup>H NMR (400 MHz) spectrum of 3 (C<sub>6</sub>D<sub>6</sub>).

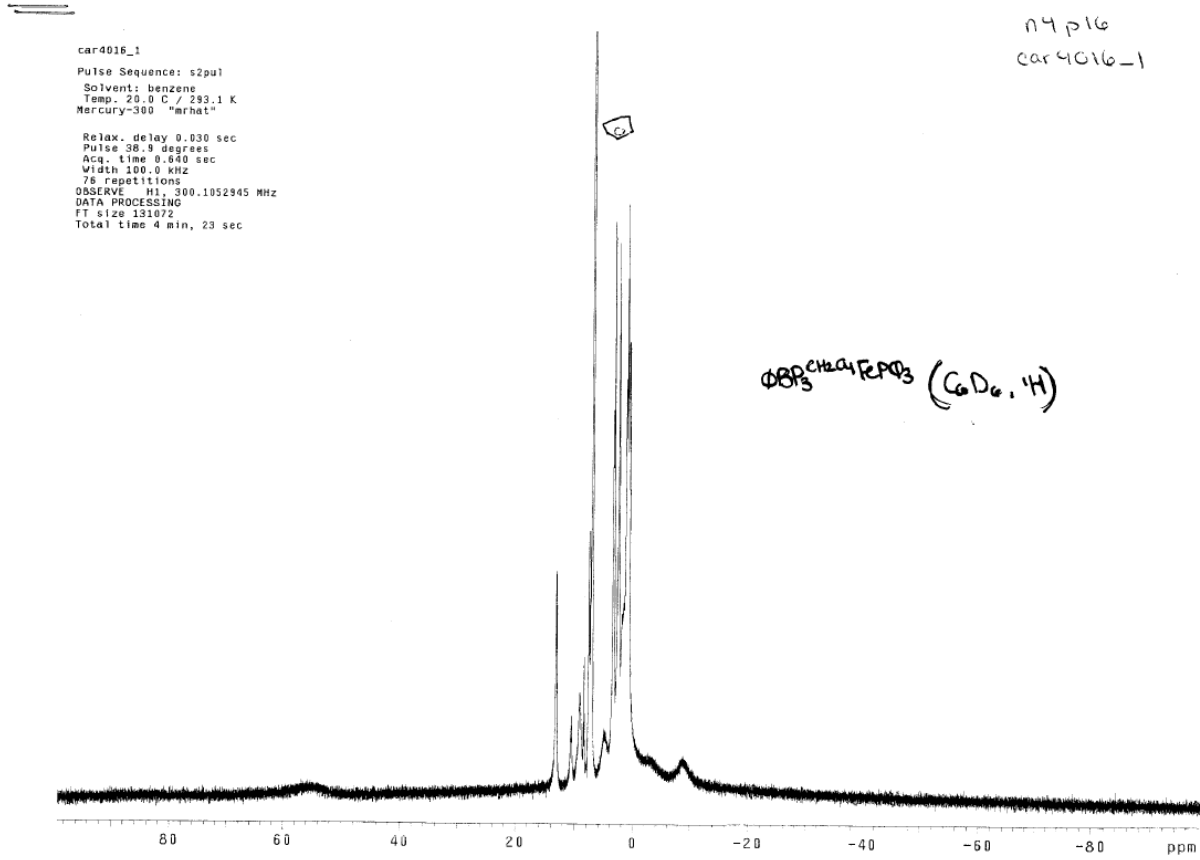


Fig. S6.  $^1\text{H}$  NMR (300 MHz) spectrum of **7** ( $\text{C}_6\text{D}_6$ ).

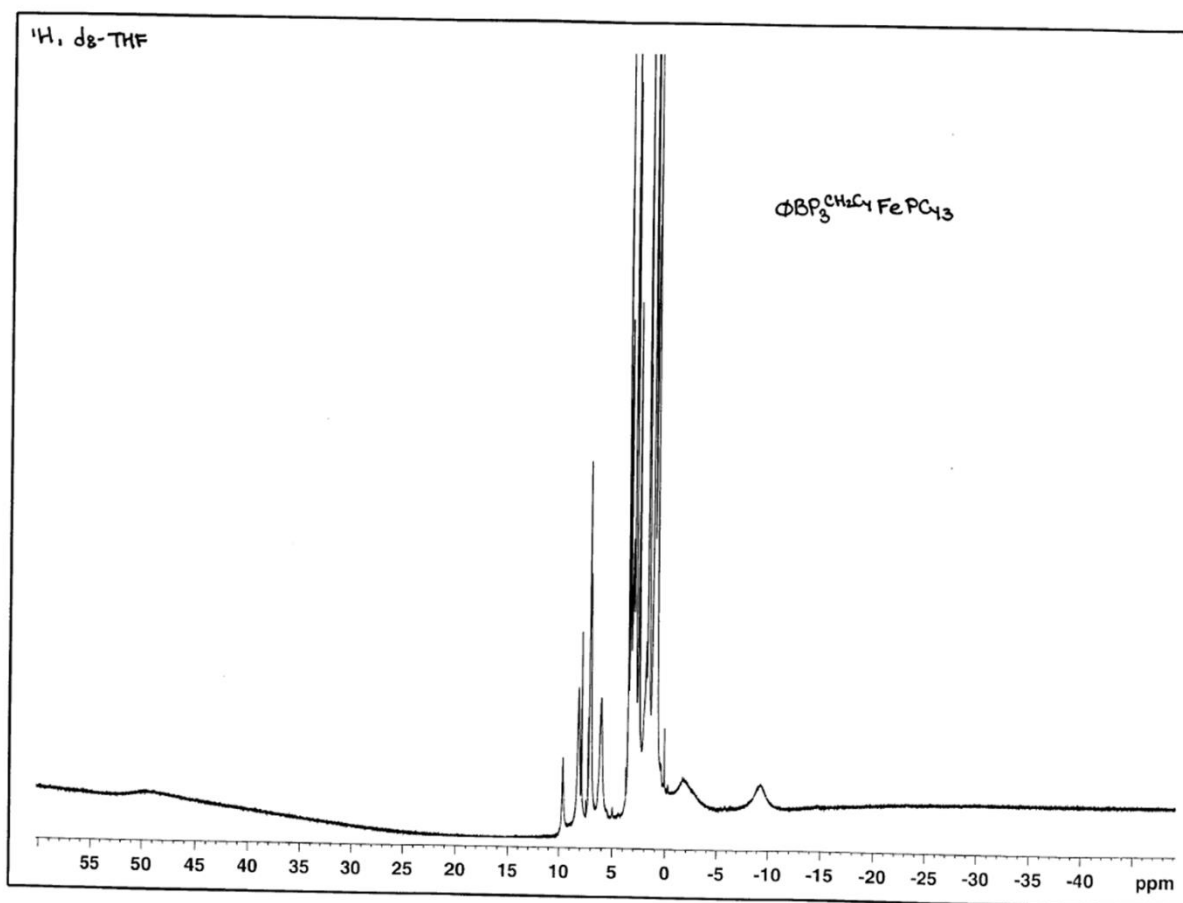
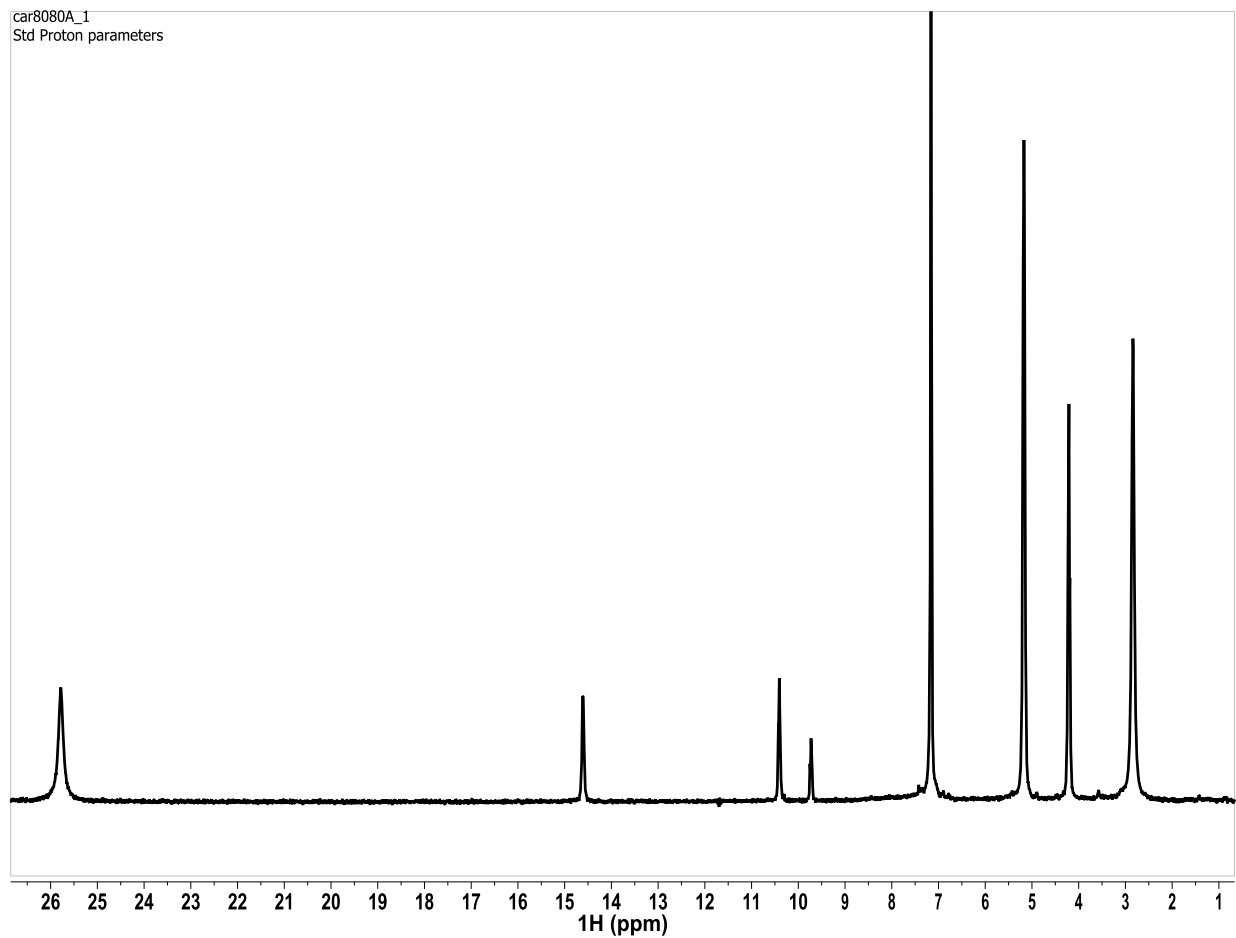
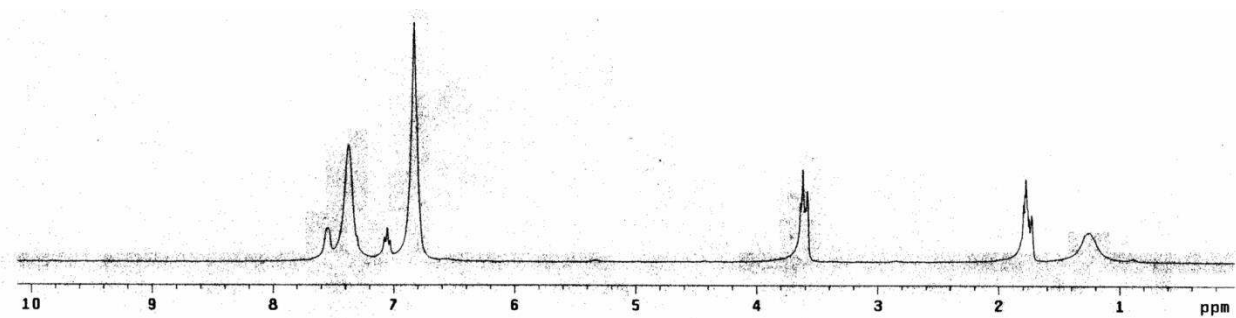


Fig. S7.  $^1\text{H}$  NMR (400 MHz) spectrum of **8** ( $d_8$ -THF).



**Fig. S8.**  $^1\text{H}$  NMR (300 MHz) spectrum of **12** ( $\text{C}_6\text{D}_6$ ).



**Fig. S9.**  $^1\text{H}$  NMR (300 MHz) spectrum of **14** ( $d_8$ -THF).

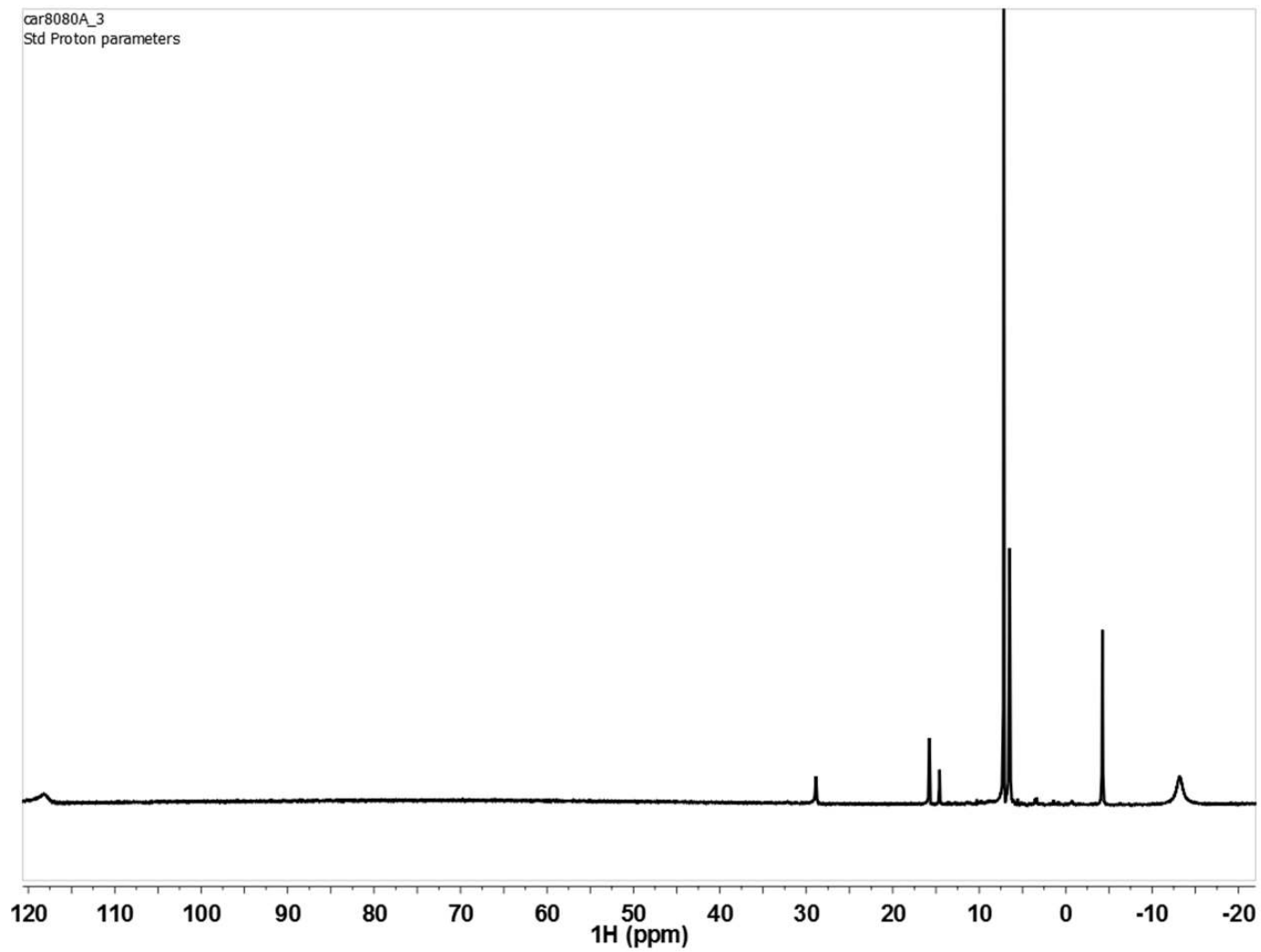


**Fig. S10.**  $^1\text{H}$  NMR (300 MHz) spectrum of **15** ( $\text{C}_6\text{D}_6$ ).

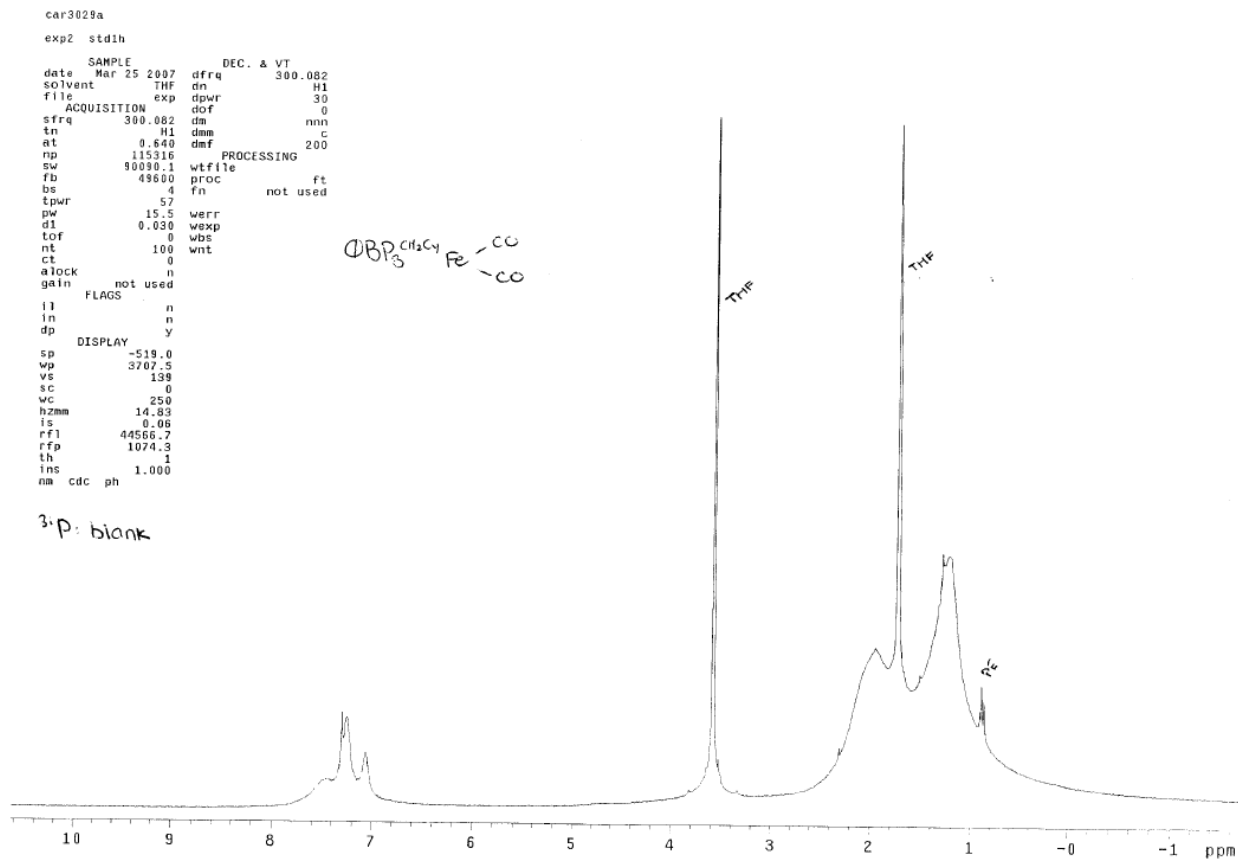
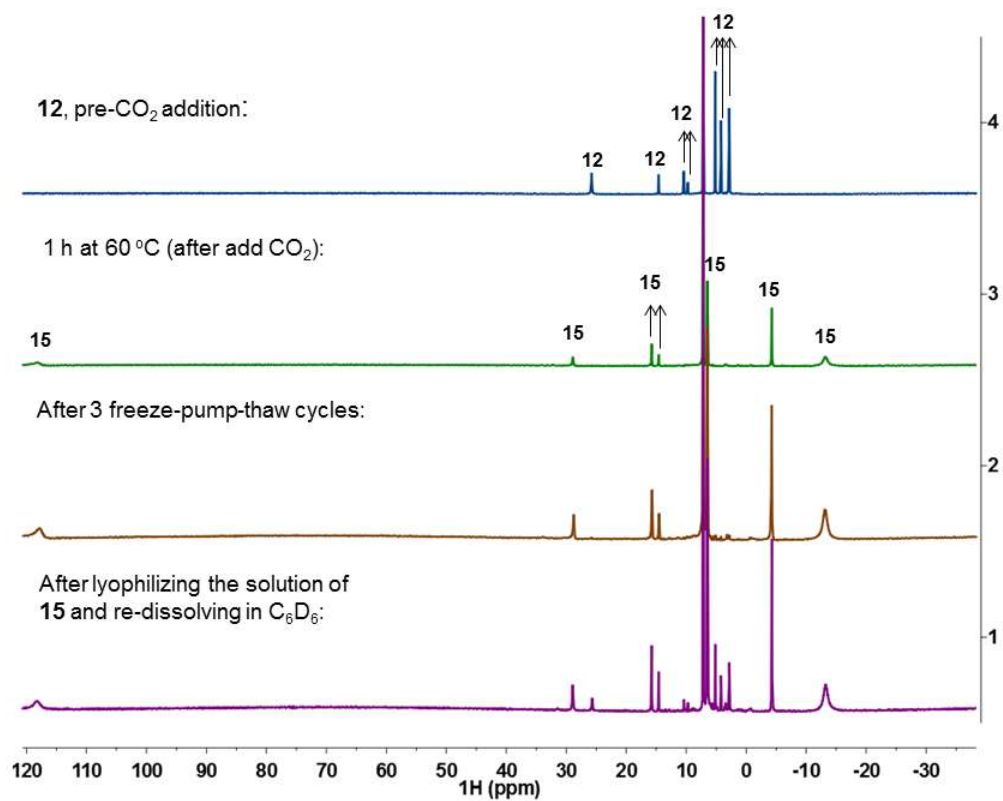
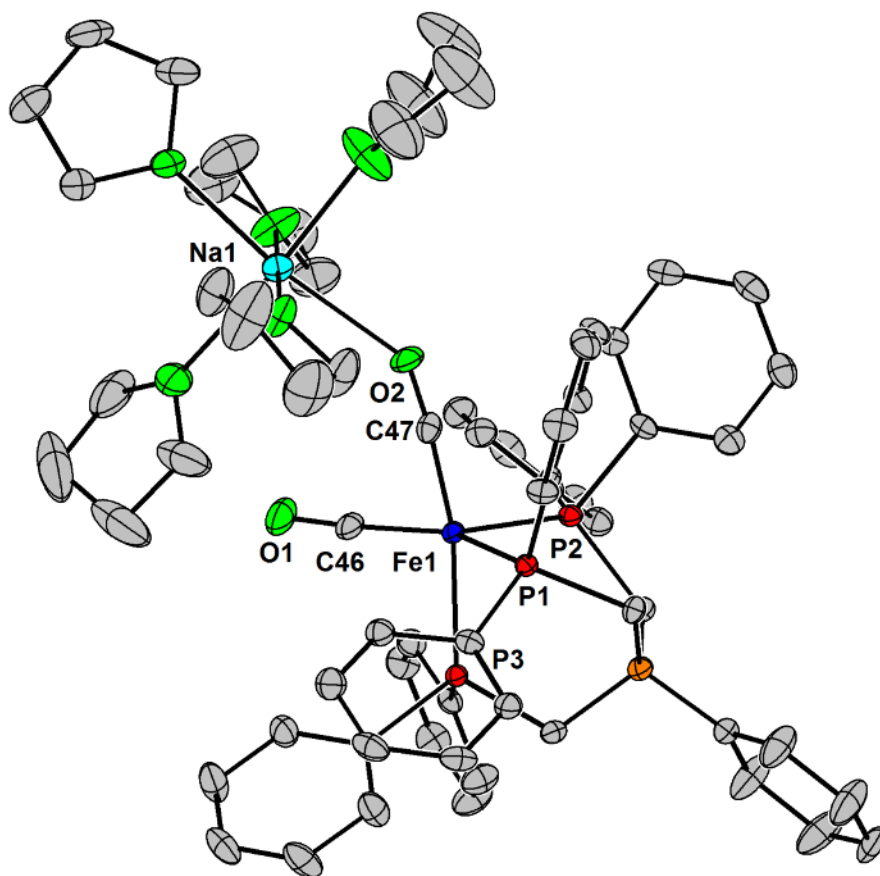


Fig. S11.  $^1\text{H}$  NMR (300 MHz) spectrum of  $[\text{PhBP}^{\text{CH}_2\text{Cy}}_3\text{Fe}(\text{CO})_2]$  ( $\text{C}_6\text{D}_6$ ).





**Fig. S12.**  $^1\text{H}$  NMR profile ( $\text{C}_6\text{D}_6$ ) of the reaction between **12** and  $\text{CO}_2$ .



**Fig. S13.** 50% thermal ellipsoid representation of  $\{[\text{PhBP}^{\text{Ph}}_3]\text{Fe}(\text{CO})_2\}\{\text{Na}(\text{THF})_5\}$  (**14**). Hydrogen atoms have been removed for clarity. Selected bond distances ( $\text{\AA}$ ) and angles (deg.) for **6.13**: Fe1-P1 2.2158(8), Fe1-P2 2.2116(8), Fe1-P3 2.2663(8), Fe1-C47 1.750(3), Fe1-C46 1.752(3), C46-O1 1.162(4), C47-O2 1.158(3), O2-Na1 2.501(2), C47-Fe1-C46 82.7(1), C47-Fe1-P2 103.9(1), C46-Fe1-P2 121.6(1), C47-Fe1-P1 93.75(9), C46-Fe1-P1 143.7(1), P2-Fe1-P1 94.35(3), C47-Fe1-P3 167.4(1), C46-Fe1-P3 89.30(9), P2-Fe1-P3 88.50(3), P1-Fe1-P3 86.97(3).

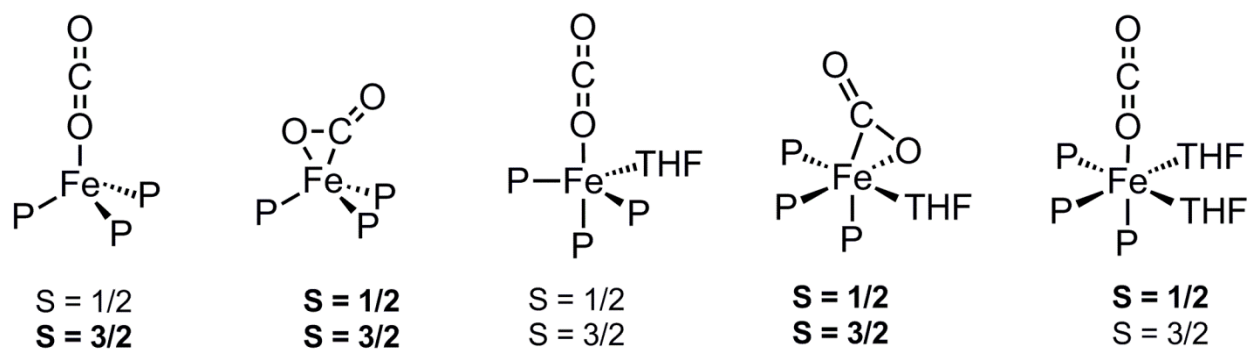


**Fig S14.**  $[\text{PhBP}^{\text{Me}}_3]\text{Fe}(\text{CO}_2)(\text{THF})_x$  structures and spin-states that were investigated by DFT methods. The structures/spin-states that could satisfactorily be minimized are bolded. Geometry optimizations on  $\eta^2\text{-OCO}$  and  $\eta^1\text{-CO}_2$  species both minimized to the  $\eta^2\text{-OCO}$  bonding mode.

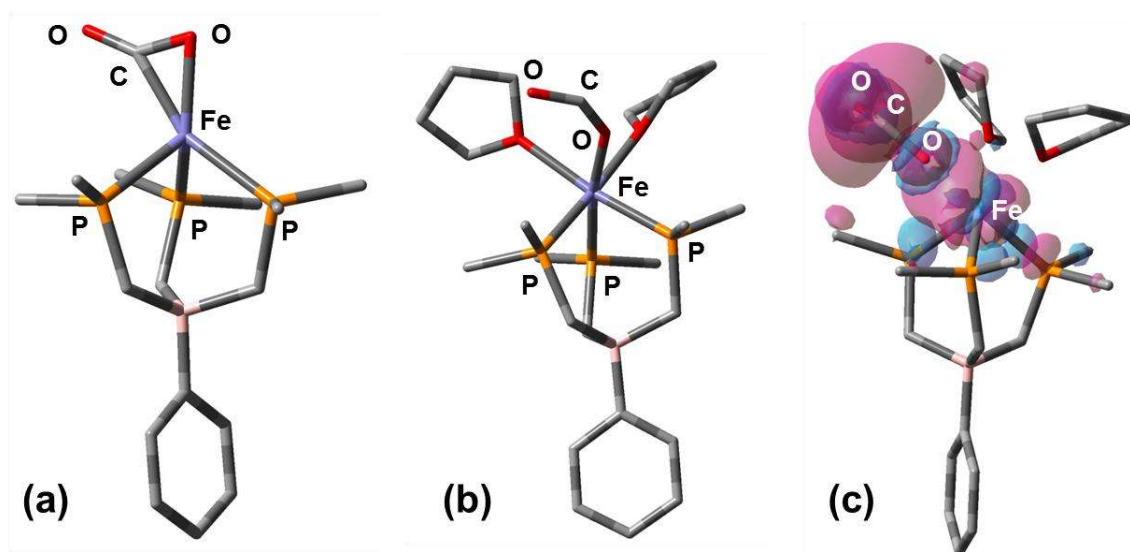


**Fig. 15.** Theoretically predicted geometry (DFT, B3LYP/6-311++G\*\*) for (a)  $\text{Fe}(\eta^2\text{-OCO})$  quartet (b)  $\text{Fe}(\eta^1\text{-OCO})(\text{THF})_2$  doublet, and (c) the calculated spin-density of  $\text{Fe}(\eta^1\text{-OCO})(\text{THF})_2$ . Calculated bond distances (Å) and angles for  $\text{Fe}(\eta^2\text{-OCO})$  ( $S = 3/2$ ): Fe-O, 2.02; Fe-C, 2.00; O-C (bound), 1.25; O-C (distal), 1.20; O-C-O,  $143.5^\circ$ . Calculated bond distances (Å) and angles for  $\text{Fe}(\eta^1\text{-OCO})(\text{THF})_2$  ( $S = 1/2$ ): Fe-O, 2.04; Fe- $\text{THF}_{\text{ave}}$ , 2.25; O-C (bound), 1.26; O-C (distal), 1.22; O-C-O,  $136.0^\circ$ .

**Table S1.** Cartesian coordinates of the UB3LYP/(TZVP/SV) optimized geometry of [PhBP<sup>Me</sup><sub>3</sub>]Fe( $\eta^1$ -OCO) quartet. The TZVP basis set was used for the Fe, P, B, and CO<sub>2</sub> atoms, and SV was employed for all other atoms.

Fe	-0.67558	0.21125	-1.24395
P	1.59897	-0.3745	-1.13836
P	-0.67061	2.09594	0.15972
P	-1.54154	-1.38333	0.2471
C	0.47422	1.56019	1.52386
C	1.48764	-0.15354	3.26449
C	-2.22818	2.58466	1.05211
C	1.82435	-0.75266	0.66793
C	-0.67966	-0.96249	1.84061
C	-0.04695	3.77654	-0.34539
C	-3.34133	-1.50919	0.7085
C	-1.1495	-3.18333	-0.01014
C	0.89974	-0.73005	4.41927
C	3.41642	0.44818	4.70267
C	2.89689	0.90938	-1.49395
C	2.34087	-1.83565	-2.02167
B	0.75132	-0.08575	1.78538
C	2.80488	-0.1402	5.82387
C	2.7659	0.43757	3.45797
C	1.53969	-0.72855	5.67352
H	0.10221	2.01992	2.46337
H	1.45226	2.04427	1.31699
H	-2.66035	1.69966	1.55205
H	-2.0169	3.35246	1.82092
H	1.76246	-1.85783	0.765
H	2.87057	-0.48863	0.92314
H	-0.50809	-1.92451	2.36667
H	-1.41681	-0.40217	2.45439
H	0.92899	3.67151	-0.85363
H	-0.75307	4.25627	-1.04985
H	-3.48195	-2.16758	1.58726
H	-3.73274	-0.50508	0.95392
H	-0.06009	-3.30841	-0.14173
H	-1.65734	-3.56387	-0.91634
H	2.68042	1.82542	-0.91633
H	2.89872	1.16715	-2.56981
H	1.70206	-2.72468	-1.86974
H	-0.08755	-1.19585	4.35077
H	1.0452	-1.18983	6.53625
H	3.3068	-0.13829	6.79718
H	4.40308	0.91579	4.79934
H	3.27292	0.90887	2.6074
O	-1.7776	0.42851	-3.29295
C	-2.64056	0.7306	-4.01279
O	-3.49455	1.02797	-4.73449
H	3.35444	-2.05807	-1.63619
H	2.40393	-1.63774	-3.10865
H	3.90248	0.54473	-1.20862

H	0.08253	4.43323	0.53637
H	-2.97504	2.9841	0.34019
H	-3.92876	-1.9115	-0.13894
H	-1.46824	-3.78573	0.8621

**Table S2.** Cartesian coordinates of the UB3LYP/(TZVP/SV) optimized geometry of  $[\text{PhBP}^{\text{Mc}}_3\text{Fe}(\eta^2\text{-OCO})$  quartet. The TZVP basis set was used for the Fe, P, B, and  $\text{CO}_2$  atoms, and SV was employed for all other atoms.

Fe	6.4535	9.66207	8.26994
P	5.51778	11.31747	9.79636
P	4.38343	8.36868	8.1585
P	7.34392	8.30081	10.07043
C	3.61235	8.46034	9.84344
O	9.10887	11.11372	7.85016
C	3.63851	8.40239	12.49105
C	4.54457	6.55237	7.81854
C	4.981	10.4137	11.31931
C	5.95928	7.82568	11.1979
C	3.03875	8.82769	6.96416
C	8.2515	6.74146	9.64645
C	8.11107	10.5299	7.54795
C	8.57995	9.1646	11.14285
C	3.90389	7.32538	13.37433
C	1.59083	8.82717	13.82191
C	4.00826	12.22097	9.21488
C	6.59136	12.71786	10.35581
B	4.57867	8.78034	11.18964
C	1.89023	7.75557	14.68145
C	2.44984	9.13541	12.75446
C	3.05295	7.00497	14.44931
H	3.07707	7.50175	10.00461
H	2.82355	9.23938	9.78726
H	5.21838	6.0892	8.5603
H	3.55901	6.05369	7.8839
H	5.80618	10.50494	12.05657
H	4.13535	10.98914	11.74604
H	6.38764	7.7902	12.22039
H	5.67543	6.7831	10.94351
H	2.78328	9.89613	7.08046
H	3.38012	8.66779	5.92437
H	8.53455	6.19523	10.56618
H	7.6127	6.08661	9.02751
H	8.1307	10.07004	11.58571
H	9.45269	9.4718	10.53888
H	3.20484	11.50445	8.97197
H	4.24035	12.81155	8.30997
H	7.54809	12.32538	10.7425
H	6.82253	13.38158	9.50254
O	7.46628	10.07744	6.57524
H	4.79621	6.7095	13.22958
H	3.30165	6.16455	15.10719
H	1.22664	7.51062	15.51716
H	0.68587	9.42348	13.98437
H	2.18083	9.97586	12.10321
H	9.16494	6.97971	9.07116
H	4.9674	6.38711	6.8103

H	2.12954	8.2233	7.14431
H	3.64309	12.90149	10.00729
H	6.09315	13.30298	11.15178
H	8.91046	8.5005	11.96357

**Table S3.** Cartesian coordinates of the UB3LYP/(TZVP/SV) optimized geometry of [PhBP<sup>Me</sup><sub>3</sub>]Fe( $\eta^2$ -OCO) doublet. The TZVP basis set was used for the Fe, P, B, and CO<sub>2</sub> atoms, and SV was employed for all other atoms.

Fe	5.62612	9.80569	8.50284
P	4.90582	11.23731	10.05929
P	3.64501	8.45812	8.55761
P	6.70462	8.60315	10.08699
C	2.99249	8.38583	10.28372
O	8.23988	11.29521	8.21074
C	3.3443	8.27479	12.9131
C	3.88405	6.6833	8.07197
C	4.39013	10.38613	11.61072
C	5.52534	7.89815	11.3161
C	2.21649	8.91889	7.46424
C	7.63145	7.1953	9.3164
C	7.18352	10.78728	7.95001
C	8.0246	9.42087	11.08572
C	3.79362	7.2066	13.72984
C	1.46107	8.53719	14.502
C	3.41131	12.16205	9.47268
C	6.02708	12.62757	10.53364
B	4.08183	8.73391	11.51689
C	1.93952	7.47613	15.29069
C	2.15291	8.9202	13.34142
C	3.11083	6.81151	14.89592
H	2.55268	7.37975	10.44117
H	2.1483	9.10361	10.34673
H	4.59546	6.19597	8.76084
H	2.92315	6.13728	8.12405
H	5.19266	10.54819	12.35994
H	3.50004	10.92419	11.9927
H	6.0705	7.85451	12.28
H	5.31235	6.84869	11.02658
H	1.90569	9.96039	7.65988
H	2.51148	8.84312	6.40106
H	8.06786	6.54809	10.10005
H	6.95556	6.58678	8.69016
H	7.5718	10.13157	11.79822
H	8.71027	9.97463	10.42043
H	2.56684	11.46844	9.32174
H	3.62771	12.6737	8.51733
H	6.99114	12.23266	10.89367
H	6.23588	13.26054	9.65268
O	6.43502	10.61077	6.93001
H	4.69978	6.65758	13.45663
H	3.49713	5.98041	15.49666
H	1.40618	7.17269	16.19746
H	0.54674	9.06657	14.79285
H	1.74675	9.74948	12.74957
H	8.44427	7.58677	8.67759



H	4.28313	6.61311	7.04324
H	1.35396	8.25114	7.64951
H	3.11583	12.91581	10.22635
H	5.56232	13.23996	11.32869
H	8.58692	8.66368	11.66333

**Table S4.** Cartesian coordinates of the UB3LYP/(TZVP/SV) optimized geometry of  $[\text{PhBP}^{\text{Mc}}_3]\text{Fe}(\eta^2\text{-OCO})(\text{THF})$  doublet. The TZVP basis set was used for the Fe, P, B, and  $\text{CO}_2$  atoms, and SV was employed for all other atoms.

Fe	-0.74331	0.61306	-1.26735
P	1.24226	-0.41999	-0.8459
P	-0.25596	2.2077	0.36127
P	-1.76146	-0.83069	0.43146
C	0.73849	1.52441	1.76163
O	-0.38817	0.46012	-3.24819
C	1.35893	-0.36681	3.51823
C	-1.73827	2.93903	1.20992
C	1.51245	-0.98051	0.88697
C	-0.92912	-0.6568	2.07507
C	0.62142	3.7443	-0.17987
C	-3.57014	-0.61199	0.80226
C	-0.03424	1.58349	-2.78568
C	-1.72497	-2.65982	0.10177
C	0.64301	-0.75627	4.67883
C	3.379	-0.26106	4.94974
C	2.76076	0.56261	-1.24765
C	1.48588	-1.8906	-1.94516
B	0.65473	-0.12972	2.05025
C	2.63742	-0.65286	6.07821
C	2.74645	-0.1231	3.70321
C	1.26303	-0.89899	5.93466
H	0.43542	2.07591	2.67489
H	1.7976	1.79872	1.57663
H	-2.2954	2.15575	1.75162
H	-1.4099	3.69945	1.94318
H	1.24293	-2.05473	0.95439
H	2.60166	-0.92718	1.08036
H	-0.99607	-1.64567	2.57343
H	-1.5463	0.03873	2.68116
H	1.56035	3.47514	-0.69097
H	0.00898	4.3043	-0.90823
H	-3.85301	-1.20831	1.69017
H	-3.78904	0.4515	1.0009
H	-0.68218	-3.01594	0.05024
H	-2.22179	-2.88895	-0.85913
H	2.70202	0.95883	-2.2765
H	0.67185	-2.62014	-1.79096
H	1.4611	-1.56591	-3.00016
O	0.42699	2.61619	-3.20688
H	-0.43117	-0.95418	4.6126
H	0.66826	-1.20362	6.80343
H	3.12412	-0.76331	7.05288
H	4.4528	-0.06239	5.04235
H	3.35698	0.18821	2.84695
H	-4.18733	-0.93602	-0.05552
H	-2.23905	-3.20685	0.91459

H	2.86161	1.41348	-0.55182
H	3.6587	-0.07602	-1.15041
H	2.45281	-2.38086	-1.72696
H	-2.41514	3.41405	0.47924
H	0.84375	4.38372	0.69454
C	-3.42117	0.46581	-2.79526
O	-2.68085	1.36712	-1.88292
C	-2.95407	2.77196	-2.25403
C	-3.58033	2.71141	-3.65147
C	-4.35143	1.37188	-3.61595
H	-2.6793	-0.04852	-3.42901
H	-3.95577	-0.27	-2.17232
H	-3.65669	3.18441	-1.50495
H	-2.00461	3.32582	-2.21934
H	-4.23346	3.57746	-3.85396
H	-2.79189	2.68912	-4.42528
H	-5.3278	1.49878	-3.11194
H	-4.54164	0.96222	-4.62259

**Table S5.** Cartesian coordinates of the UB3LYP/(TZVP/SV) optimized geometry of  $[\text{PhBP}^{\text{Mc}}_3]\text{Fe}(\eta^2\text{-OCO})(\text{THF})$  quartet. The TZVP basis set was used for the Fe, P, B, and  $\text{CO}_2$  atoms, and SV was employed for all other atoms.

Fe	6.4535	9.66207	8.26994
P	5.51778	11.31747	9.79636
P	4.38343	8.36868	8.1585
P	7.34392	8.30081	10.07043
C	3.61235	8.46034	9.84344
O	9.10887	11.11372	7.85016
C	3.63851	8.40239	12.49105
C	4.54457	6.55237	7.81854
C	4.981	10.4137	11.31931
C	5.95928	7.82568	11.1979
C	3.03875	8.82769	6.96416
C	8.2515	6.74146	9.64645
C	8.11107	10.5299	7.54795
C	8.57995	9.1646	11.14285
C	3.90389	7.32538	13.37433
C	1.59083	8.82717	13.82191
C	4.00826	12.22097	9.21488
C	6.59136	12.71786	10.35581
B	4.57867	8.78034	11.18964
C	1.89023	7.75557	14.68145
C	2.44984	9.13541	12.75446
C	3.05295	7.00497	14.44931
H	3.07707	7.50175	10.00461
H	2.82355	9.23938	9.78726
H	5.21838	6.0892	8.5603
H	3.55901	6.05369	7.8839
H	5.80618	10.50494	12.05657
H	4.13535	10.98914	11.74604
H	6.38764	7.7902	12.22039
H	5.67543	6.7831	10.94351
H	2.78328	9.89613	7.08046
H	3.38012	8.66779	5.92437
H	8.53455	6.19523	10.56618
H	7.6127	6.08661	9.02751
H	8.1307	10.07004	11.58571
H	9.45269	9.4718	10.53888
H	3.20484	11.50445	8.97197
H	4.24035	12.81155	8.30997
H	7.54809	12.32538	10.7425
H	6.82253	13.38158	9.50254
O	7.46628	10.07744	6.57524
H	4.79621	6.7095	13.22958
H	3.30165	6.16455	15.10719
H	1.22664	7.51062	15.51716
H	0.68587	9.42348	13.98437
H	2.18083	9.97586	12.10321
H	9.16494	6.97971	9.07116

H	4.9674	6.38711	6.8103
H	2.12954	8.2233	7.14431
H	3.64309	12.90149	10.00729
H	6.09315	13.30298	11.15178
H	8.91046	8.5005	11.96357

**Table S6.** Cartesian coordinates of the UB3LYP/6-31++g(d,p) optimized geometry of [PhBP<sup>Me</sup><sub>3</sub>]Fe( $\eta^1$ -OCO)(THF)<sub>2</sub> doublet.

Fe	-0.70463	0.31794	-1.25602
P	1.13711	-1.03279	-0.90423
P	0.17743	1.92671	0.19404
P	-1.67228	-0.66125	0.59461
C	1.26335	1.22941	1.50967
C	1.69754	-0.5786	3.42167
C	-1.06607	2.87993	1.20556
C	1.48576	-1.41905	0.87128
C	-0.72791	-0.53991	2.17505
C	1.15948	3.3794	-0.44312
C	-3.3879	-0.08798	1.02701
C	-2.00532	-2.47413	0.41577
C	1.04548	-0.80513	4.65012
C	3.81928	-0.70471	4.67437
C	2.77855	-0.40354	-1.51164
C	1.14368	-2.68427	-1.73841
B	0.91482	-0.33293	1.99861
C	3.13572	-0.93338	5.87308
C	3.10762	-0.53303	3.48443
C	1.74071	-0.9814	5.85335
H	1.22626	1.92918	2.35605
H	2.29466	1.27525	1.13204
H	-1.63539	2.20942	1.84979
H	-0.53248	3.5901	1.84588
H	1.0645	-2.41419	1.07043
H	2.57347	-1.54636	0.94927
H	-0.95104	-1.46095	2.73129
H	-1.16854	0.27627	2.76387
H	2.09457	3.03909	-0.89333
H	0.60325	3.94999	-1.19323
H	-3.66866	-0.49436	2.00417
H	-3.43718	1.00186	1.06589
H	-1.06992	-3.036	0.39492
H	-2.54678	-2.6599	-0.5137
H	3.0305	0.56115	-1.06373
H	2.77074	-0.30587	-2.59999
H	0.26563	-3.26146	-1.44149
H	1.11098	-2.56992	-2.82356
H	-0.04069	-0.84759	4.68155
H	1.18966	-1.15689	6.77486
H	3.68135	-1.07143	6.80288
H	4.90636	-0.66259	4.66768
H	3.67521	-0.35506	2.5719
O	-1.71288	-1.06491	-2.36424
C	-1.61928	-1.81016	-3.37665
O	-0.77013	-2.04562	-4.22107
H	3.5578	-1.12114	-1.23468
H	2.04423	-3.23143	-1.43927

H	1.40804	4.04127	0.39288
H	-1.76903	3.43326	0.57849
H	-4.10705	-0.44272	0.28415
H	-2.59425	-2.82299	1.27058
C	-3.72877	1.02274	-2.28824
O	-2.50406	1.55696	-1.72837
C	-2.50862	2.94614	-2.10694
C	-3.95404	3.41315	-1.87554
C	-4.78456	2.10603	-2.01682
H	-3.58364	0.8598	-3.36317
H	-3.91438	0.05855	-1.82411
H	-1.76143	3.46326	-1.50855
H	-2.23037	3.03307	-3.16467
H	-4.0688	3.84042	-0.8752
H	-4.24549	4.18009	-2.59864
H	-5.33332	1.8937	-1.09525
H	-5.5131	2.15882	-2.83059
O	0.01862	1.24626	-3.21454
C	-0.66152	1.14302	-4.48836
C	1.23108	1.96851	-3.51395
C	0.43777	0.78386	-5.48879
H	-1.44256	0.39549	-4.39742
H	-1.10657	2.12204	-4.7236
C	1.70043	1.46135	-4.89223
H	0.99953	3.0427	-3.54667
H	1.93498	1.78612	-2.70779
H	0.20146	1.14242	-6.49478
H	0.54786	-0.3017	-5.52416
H	2.06122	2.29102	-5.50736
H	2.52118	0.74524	-4.7946

**Table S7.** Mulliken atomic spin densities (UB3LYP/6-31++g(d,p)) of the  $[\text{PhBP}^{\text{Me}}_3]\text{Fe}(\text{CO}_2)(\text{THF})_x$  species that could be satisfactorily minimized.

	$[\text{PhBP}^{\text{Me}}_3]\text{Fe}$ ( $\eta^1\text{-CO}_2$ ) $S = 3/2$	$[\text{PhBP}^{\text{Me}}_3]\text{Fe}$ ( $\eta^2\text{-CO}_2$ ) $S = 3/2$	$[\text{PhBP}^{\text{Me}}_3]\text{Fe}$ ( $\eta^2\text{-CO}_2$ ) $S = 1/2$	$[\text{PhBP}^{\text{Me}}_3]\text{Fe}$ ( $\eta^2\text{-CO}_2$ )(THF) $S = 1/2$	$[\text{PhBP}^{\text{Me}}_3]\text{Fe}$ ( $\eta^2\text{-CO}_2$ )(THF) $S = 3/2$	$[\text{PhBP}^{\text{Me}}_3]\text{Fe}$ ( $\eta^1\text{-CO}_2$ )(THF) <sub>2</sub> $S = 1/2$
<b>Fe</b>	2.870217	3.142604	1.099547	1.055221	3.038812	0.284236
<b>O<sub>prox</sub></b>	-0.003366	0.026957	0.026649	0.026543	-0.103372	-0.10424
<b>C</b>	0.004623	-0.2644	-0.06345	-0.064401	-0.294548	0.771407
<b>O<sub>dist</sub></b>	0.002616	-0.0957	-0.01371	-0.020867	0.036996	0.155375
<b><math>[\text{PhBP}^{\text{Me}}_3]^- / \text{THF}</math></b>	0.12591	0.190541	-0.04904	0.003504	0.322112	-0.10678



## References

- 1 F. Neese, *QCPE Bull.*, 1995, **15**, 5.
- 2 E. M. Schubert, *J. Chem. Educ.*, 1992, **69**, 62.
- 3 G. M. Sheldrick, *Acta Cryst.*, 1990, **A46**, 467-473.
- 4 G. M. Sheldrick, *Acta Cryst.*, 2008, **A64**, 112-122.
- 5 P. Müller, R. Herbst-Irmer, A. L. Spek, T. R. Schneider and M. R. Sawaya, *Crystal Structure Refinement: A Crystallographer's Guide to SHELXL*, Oxford University Press, Oxford, 2006.
- 6 A. L. Spek, Utrecht University, Utrecht, Holland, 2008.
- 7 M. J. Frisch, G. W. Trucks, H. B. Schlegel, G. E. Scuseria, M. A. Robb, J. R. Cheeseman, J. A. Montgomery, T. Vreven, K. N. Kudin, J. C. Burant, J. M. Millam, S. S. Iyengar, J. Tomasi, V. Barone, B. Mennucci, M. Cossi, G. Scalmani, N. Rega, G. A. Petersson, H. Nakatsuji, M. Hada, M. Ehara, K. Toyota, R. Fukuda, J. Hasegawa, M. Ishida, T. Nakajima, Y. Honda, O. Kitao, H. Nakai, M. Klene, X. Li, J. E. Knox, H. P. Hratchian, J. B. Cross, V. Bakken, C. Adamo, J. Jaramillo, R. Gomperts, R. E. Stratmann, O. Yazyev, A. J. Austin, R. Cammi, C. Pomelli, J. W. Ochterski, P. Y. Ayala, K. Morokuma, G. A. Voth, P. Salvador, J. J. Dannenberg, V. G. Zakrzewski, S. Dapprich, A. D. Daniels, M. C. Strain, O. Farkas, D. K. Malick, A. D. Rabuck, K. Raghavachari, J. B. Foresman, J. V. Ortiz, Q. Cui, A. G. Baboul, S. Clifford, J. Cioslowski, B. B. Stefanov, G. Liu, A. Liashenko, P. Piskorz, I. Komaromi, R. L. Martin, D. J. Fox, T. Keith, A. Laham, C. Y. Peng, A. Nanayakkara, M. Challacombe, P. M. W. Gill, B. Johnson, W. Chen, M. W. Wong, C. Gonzalez and J. A. Pople, *Gaussian 03, Revision C.02*, Gaussian, Inc., Wallingford, CT, 2004.
- 8 D. C. Young, *Spin Contamination*, John Wiley & Sons, Inc., 2002.
- 9 R. I. Dennington, T. Keith and J. Millam, Semichem, Inc., Shawnee Mission, KS, 2007.
- 10 (a) C. C. Lu, C. T. Saouma, M. W. Day and J. C. Peters, *J. Am. Chem. Soc.*, 2007, **129**, 4-5; (b) C. T. Saouma, C. C. Lu and J. C. Peters, *Inorg. Chem.*, 2012, **51**, 10043-10054; (c) S. D. Brown, T. A. Betley and J. C. Peters, *J. Am. Chem. Soc.*, 2003, **125**, 322-323; (d) T. A. Betley and J. C. Peters, *Inorg. Chem.*, 2003, **42**, 5074-5084; (e) T. A. Betley and J. C. Peters, *J. Am. Chem. Soc.*, 2003, **125**, 10782-10783.